LOW-NOISE CABLE FOR DIAGNOSTICS, CONTROL AND INSTRUMENTATION OF THE ASDEX TOKAMAK FUSION EXPERIMENT

Joachim Gernhardt

IPP III/67 November 1988

MAX-PLANCK-INSTITUT FÜR PLASMAPHYSIK

8046 GARCHING BEI MÜNCHEN

LOW-NOISE CABLE FOR DIAGNOSTICS, CONTROL AND INSTRUMENTATION OF THE ASDEX TOKAMAK FUSION EXPERIMENT

Joachim Gernhardt

IPP III/67 November 1988

Low-noise Cable for Diagnostics, Control and Instrumentation in the ASDEX (Tokamak) Fusion Experiment

Abstract

ASDEX (Axially Symmetric Divertor EXperiment) is a large tokamak (R = 1.65 m; a = 0.4 m) with an air transformer. The relatively large stray field,

$$B_z = 10\ \text{mT} = (100\ \text{G});\ \text{for}\ \rho = 5\ \text{m},$$
$$B_z = 40\ \text{mT} = (400\ \text{G});\ \text{for}\ \rho = 3\ \text{m},$$
$$B_\phi = 0.3\ \text{T} = (3\ \text{kG});\ \text{for}\ \rho = 3\ \text{m},$$

compared with that of an iron transformer (for notation see /1/), and the cable length $l \geq 30$ m from the experiment to the control room, make mainly the magnetically induced and capacitively coupled noise signal in the cable relatively high. As a result of neutral injection (>4 MW; 40 kV) and lower hybrid ion cyclotron and Alfven wave heating strong E-fields are produced and noise is coupled into the cables. These magnetic and electric field gradients during the plasma shot vary with time and location. This report tries to show how these noise signals can be reduced without reducing the broadcast frequency of the signal. The Electro Magnetic Compatibility and Interference (EMC, EMI) are discussed. The cost of diagnostic cable, connectors and cable ducts without mounting is approximately DM 700,000.--.

Table of Contents

Section No.	Title	Page No.
	Abstract	1
	Table of Contents	2
1	Introduction	3
2	Pick-up Noise	3
3	Electromagnetic Interference (EMI)	6
4	Cable Test in our Workshop with a Time Varying Magnetic Field	14
5	Induced Voltage in Cables Measured in ASDEX during a 30 kA Ohmic Heating Pulse	16
6	Twisted Pair	17
7	Calculation of a Double Magnetic Shell and its Efficiency as a Magnetic Shield for a Coaxial Cable with 12 Conductors against External Magnetic Fields	17
8	Shielding	19
9	Common-mode Impedance Coupling	20
10	Special Cable Arrangements for High Temperatures and High-vacuum Conditions	20
11	Example of an Electric Circuit in an Experimental Environment	21
12	Noise Reduction	22
13	Typical Damage Energies of Electronic Components	24
14	Overvoltage Protection	24
15	Appendix A: Decibels	26
16	Appendix B: Insulation Material for Cables	28
17	Appendix C: a New Special Cable for High-vacuum Conditions	29
18	References	30
19	Figure Captions	31

1. Introduction

As tokamaks increase in size, the iron transformers for the ohmic heating system are superseded by air transformers. At the same time the energy levels of the poloidal and toroidal coil systems and the additional heating power from NI, ICRH and LH heating increases and therefore the electrostatically and magnetically induced noise voltage becomes large enough to be of real concern.

Berger of Switzerland have calculated that the induced noise voltage will increase as the cube of the operating voltage under identical conditions (for high-voltage switch yards).

The stray field of an air transformer as a factor of 20 as high as that of an iron transformer. Larger experiments need longer diagnostic, control and instrumentation cable and therefore the noise pick-up is correspondingly higher (function of cable length). The magnetic field is associated with high currents in the coils (~45 kA) and therefore the pick-up voltage in these cables is higher than in small experiments.

The electrostatic field is associated with high voltage (~40 kV) and therefore high electric field strength at the experiment, and for this reason the charges accumulated in the signal wire by a certain stray capacitance is quite high. The two types of noise are fundamentally different and thus require different noise reduction measures. The thyristor voltage spikes of the poloidal and toroidal power supplies are of real concern.

The cables used (about 3000 30-m lengths of cable in the ASDEX experiment) are exposed to magnetic, capacitive and electrostatic coupling and in many cases to actual potential differences, as well.

2. Pick-up Noise

The problem is to keep pick-up voltages within the capabilities of the cable and the equipment connected to it.

As the cable length increases, so also does the possibility of galvanically, capacitively and inductively coupled stray signals $X_z(t)$ being superposed on measured signals.

The origin of the pick-up noise (see Fig. 1) could be due to:

a 50 Hz, A.C. current
b Radio transmitter
c Switching operation of relays, breaker etc.
d Commutation of thyristors
e Changing of magnetic flux linked into the circuit (near-field induction)
Toroidal field, ohmic heating field, vertical field radiation, divertor coil field variation with time
f Neutrons or X-rays produced in the plasma area
g Thermo-couples formed by two different metal connections (plugs) and a temperature gradient
h Ground loops
i Galvanic connection to the cable leads
j Neutral injection noise (>3 MW; 40 kV)
k Lower hybrid heating: f_o = 1.3 GHz; 1 MW; 1 s
l Ion cyclotron heating: 32.5 and 67 MHz; 3 MW, 10 s
m Alfven wave heating: f_o = 1.3 MHz; 1 MW

To reduce the pick-up noise as far as possible, the following safeguards have to be included:

1. Cable shield grounded only at one end of the cable (no ground loops); the second side of the cable should be terminated by a capacitor to reduce standing waves.
2. Proper cable path, no closed loop around the experiment
3. Highly twisted cable (2 x AWG 24 = 2 x 0.251 mm^2 Cu, two twists per cm cable length) to reduce magnetic pick-up. Apply only a measured frequency of about 500 kHz (analogue).
4. Mu-metal superscreened multiconductor coax cable (Z = 50 ohms) is applicable up to several MHz. The magnetic field in the area of the cable should not exceed 10 mT (100 G) in air.
5. Spiral copper braid shield and aluminium foil to reduce electrostatic pick-up.
6. Cable materials should resist temperatures of up to 150 °C, e.g. Tefzel (ETFE); Teflon (PTFE, FEP), because of baking of the vacuum vessel.
7. Cable connectors with small dimensions and constant, very low contact resistance (1 mΩ), e.g. Lemo connectors of series B, size 0.

8. Mechanical cable protection, e.g. Teflon and copper tubes, wooden or plastic cable ducts (to avoid ground loops).
9. Cable outside diameter ≦ connector cable diameter (≦4.2 mm).
10. Cable with high flexibility
11. Cable insulation suitable for neutron and gamma radiation of the plasma (Teflon has a very poor gamma radiation resistivity).
12. Special cable (thermo coax cables) for ultra-high-vacuum conditions with feed-through and metallic shield.

2.1 Signal Circuit

Figure 2 shows the general circuit for the transfer of signals from the transducer (source) on the left-hand side to the transmitter (load) on the right-hand side. The output signal of the transducer could be voltages or currents. The same applies to the pick-up noise. The voltage U_{CMV}, for example, is a capacitively coupled pick-up voltage and affects both leads, inducing noise currents in the same directions in relation to ground. This voltage is called the COMMON-MODE VOLTAGE.

The pick-up voltage U_{DMV} is galvanically coupled to just one lead and imposes on the conductor impedance Z_L a noise voltage

$$U_{DMV} \approx \frac{Z_L}{Z_D + Z_L 12} U_{D1} \ .$$

This interference voltage is in series with the signal voltage e_s and is called the DIFFERENTIAL-MODE VOLTAGE U_{DMV}.

Figure 3 /2/ shows a two-box (A and B) equipment-level electromagnetic interference (EMI) situation in a fusion experiment environment. The two boxes are interconnected with two power or data and control cables to provide a simple example. Each of the numbers 1 to 29 represents either a toggle switch (open or closed) or a question yes or no if the component is to be used or not. The results of these 29 questions represent over 500,000,000 possible combinations on these two box arrangements with a relatively simple situation. This is the reason why EMI control is so complex. A computer program of DON WHITE, Virginia, USA, solves the Maxwellian equations concerning these two box problems and gives the efficiency of the circuit layout.

3. Electromagnetic Interference (EMI)

3.0 Field Theory

To prevent radiation to or from a cable, a metallic shield can reduce the EMI. The performance of shields is a function of whether the source of an EMI appears as an electric or magnetic field in the near-field induction region or as an electromagnetic field in the far-field region. This is a function of the source and receptor geometry separation (radius r) and the operating frequency (f). The criterion for far or near fields is a function of these parameters.

Far-field conditions exist if $r >> \frac{\lambda}{2\pi}$, $\lambda = \frac{c}{f} = \frac{300}{f\left[\text{MHz}\right]} \left[\text{m}\right]$.

Near-field conditions exist if $r << \frac{\lambda}{2\pi}$.

The wave impedance is $Z_0 = \frac{2\pi}{\lambda} \cdot \frac{E}{H} = \frac{U}{J} \left[\Omega\right]$.

If the source current is low, we have a case of high impedance (RF currents). The electric field attenuates more rapidly with the distance

$$E \propto \frac{1}{r^2} \text{ or } 60 \frac{\text{dB}}{\text{dec}},$$

where E is the electric field strength, than the magnetic field

$$H \propto \frac{1}{r^2} \text{ or } 40 \frac{\text{dB}}{\text{dec}}.$$

(where H is the magnetic field strength) (For more detail see Fig. 4).

It is more important to know if the electric or magnetic field in the near field region could be larger. This depends on whether we have a case of high or low-impedance field (see Fig. 5).

Figure 6 shows the wave impedance (Z) as a function of the distance (r) from the source.

3.1 Electrostatic Induction (see Fig. 7)

This is coupling via a capacitive circuit and is caused by the presence of a varying electric field such as is found in the proximity of high voltages. It is a near-field effect and not applicable to the far-field situation (distance $r < \frac{\lambda}{2\pi}$) ; see /3/.

3.2 Magnetic Induction (see Fig. 8)

Varying magnetic flux linked into a circuit, as in the manner of a transformer, will cause interference. This is sometimes referred to as near-field induction and can occur in the presence of lines carrying high current (distance $r < \frac{\lambda}{2\pi}$) .

3.3 Electromagnetic Induction (see Figs. 9, 10)

This mode is a far-field effect, to the cable as antenna, and is associated with frequencies higher than 3.2 or 3.3 (distance $r \geq \frac{\lambda}{2\pi}$) .

3.11 Electrostatic Shielding (see Figs. 11 and 12)

Electrostatic induction occurs at all frequencies. The capacitance resulting from discontinuities in the shield is independent of frequencies of up to at least 1000 MHz. Protection is achieved by surrounding the cable with a metallic layer. This may be either a braid, a tape or a solid sheath. As the shielding efficiency proportional to the surface areas of the cable covered, a braid with a high optical coverage will provide more protection than one with a lower coverage /4/.

3.21 Magnetic Shielding (see Fig. 13)

Magnetic field interference is a more common interference mechanism particularly from high-current leads. Shielding against the effects of the field can be achieved in two basic ways:

1. Circulating ground currents
2. Magnetic field deflection

In the first case the disturbing field sets up an e.m.f. in the metallic shield which on completion of the shield ground allows current flow such that the resultant magnetic field produced opposes that producing it. This technique is not recommended in fusion experiments because this large ground loop current induces in nearby cables large voltages and disturbs the measured signals in this cable. A cable shield should be grounded only at one end because of the large potential differences at the two ends (usually where the higher stray capacity to ground is). To avoid standing waves, one can terminate the non-grounded opposite cable end with a capacitor.

In the second case, the path of the field may be changed by the inclusion of magnetic materials in the cable shield. This produces a low-inductance path around the cable. Provided that the magnetic material remains unsaturated, the disturbing field inside it has a very low intensity. At low frequencies the magnetic materials are susceptible to eddy currents, which may reduce the efficiency of the shield. At high frequencies eddy currents established on the surface of a copper braid will form their own fields and these are effective in cancelling the disturbing field. This overcomes the main problem arising with magnetic materials, that their permeability is frequency-dependent and reduces to a low value above 10 kHz.

3.31 Electromagnetic Shielding

By far the main source of interference at high frequencies is electromagnetic radiation. For the best protection the cable should be completely shielded on a metallic sheath with no openings in it. Radiation may still be coupled into this type of cable because the material is not perfectly conducting and the highest induced current is on the outside surface of the shield and is diminished as a result of its thickness, resulting in a longitudinal e.m.f. proportional to the current density on the inside of the shield, thus disturbing the cable. What is more, cables of this type lose their highly desirable property of being flexible. The influence of the skin effect results in a lower current density on the inside surface at high frequencies /5/.

As already explained, the problems presented by lack of flexibility of cables with solid outer shields preclude their use for all but the most difficult shielding conditions. Their use is almost exclusively confined to a frequency range of 400 MHz to 35 GHz. Where flexibility is required, it is usual to make use of wire braids as a shield. Aluminium/Mylar tape with a drain wire is sometimes employed as a screen. However, this design is a poor shield against electromagnetic leakage and is not recommended. Tapes and braids of different materials are also used and the shielding efficiency varies considerably for different designs. We used a copper braid with 85% coverage and also aluminium/Mylar tape with 50% overlap.

3.32 Shield Requirements

It will be seen from the foregoing sub-sections that the requirements for a good shield are:

1. Low resistance
2. High permeability
3. Complete coverage
4. Light weight
5. Strength
6. Electrical connectability
7. Flexibility
8. Corrosion resistance

Although there may be other requirements as well, those listed above show the wide diversity of materials and designs that may be required to achieve the desired level of shielding.

3.33 Electromagnetic Induction

In assessing the efficiency of a shield, the generally accepted method of measuring the shielding performance is by means of the surface transfer impedance (Z_T) of a cable. This relates the open-circuit voltage generated inside the sheath to the current flowing on the outside. Although this may be measured at any frequency, it is normal to specify a frequency of 30 MHz. Test methods are described in I.E.C. 96 and B.S. 2316.

Unfortunately, the test method used for measuring surface transfer impedance only assesses the electromagnetic shielding capability of the screen. For assessment of other leakage mechanisms different approaches must be taken.

The performance of a shield against electrostatic and magnetic shielding is determined by the methods described below.

3.34 Electrostatic Induction

In poorly shielded cables with significant gaps in the shield, the capacitive leakage path can be relatively large. This capacitance, known as the "through capacity", is determined by the method described in I.E.C. 96. The capacitance value obtained allows the transfer admittance of the shield to be determined. It should be noted that although B.S. 204 describes the transfer admittance as the reciprocal of transfer impedance, it is now generally accepted that this is not a suitable definition.

It is possible - by considering the cable to be located in a situation close to a conduction plane - to determine a capacitance coupling impedance Z_F for the cable which is comparable to the surface transfer impedance and is expressed in Ω/m. The expression for Z_T is (S.S. Shelkunoff)

$$Z_T = \frac{R_{DC} \cdot u}{\cosh u - \cos u} \left[\Omega\right]$$

$$u = \frac{2d}{\delta} = d \; 2 \cdot \chi \cdot \omega \cdot \mu$$

$d\left[m\right]$ thickness of the outer coaxial conductor

$\delta\left[m\right]$ skin depth

$\omega\left[H_Z\right] = 2\pi f$ frequency

$\mu = \mu_0 \cdot \mu_r = 4\pi \cdot 15^{-7} \cdot \mu_r \left[\frac{Vs}{Am}\right]$ for Cu $\mu_r = 1$

$\chi = 5.8 \cdot 10^7 \left[\frac{1}{\Omega \cdot m}\right]$ for Cu

$R_{DC}\left[\Omega\right]$ D.C. resistance of shield per metre.

Typically the value of Z_T may be of the order of 30 mΩ/m at 30 MHz for a single-braided cable with an optical coverage of 85%. However, the use of a double braid will reduce this figure by a considerable amount because the leakage through the holes is exponentially proportional to the depth of the holes, and in a double-braided cable the holes scarcely line up on top of each other. The use of a metallic tape is valuable as a shield against this type of leakage because the metallic surface of the wrap can, under the right conditions, give 100% optical coverage. When used in conjunction with a braid, the wrap may completely obscure the holes whilst making shield termination easier.

There is one important disadvantage besides the improvements achieved by using a double braid, namely the use of a triaxial cable. In the triaxial line the two braids are separated by an insulating medium. If they are correctly terminated, a situation may arise where the outer braids act as a transmission line and resonate. This results in large voltage differences in current modes. The generated voltage will make a large contribution to the disturbance on the inner braid only.

Because of the cable shield, the capacitances to ground and between the leads are much greater. This means that a shielded cable has a low pass characteristic, and that high-frequency signals of pulses with high rise times cannot be transmitted exactly. Our twisted cable 2 x AWG24 can be used up to an analogue frequency of 500 kHz at a cable length of 30 m.

3.35 Magnetic Induction

There is no internationally recognised method of determining the efficiency of shield materials in preventing magnetic field induction, although Mil-Std-461 and Mil-Std-462 describe methods of determining shielding efficiency against magnetic fields in the 30 Hz to 50 Hz region generated within an equipment system. It is also possible to use test methods which employ coils or split toroids to induce high flux levels in cables. When using these methods, it is normal to compare the cable under test with either an unshielded cable or one with a non-magnetic shield material. Under these circumstances the shielding efficiency may be found as in dB from the relation below:

$$Se\left[\text{dB}\right] = 20 \log 10 \frac{U_1}{U_2}$$ (see Appendix A on page 26)

where U_1 is the voltage pick-up on the reference cable

U_2 is the voltage pick-up on the cable under test.

This test is only applicable for low frequencies because the cancellation of the field by induced eddy current in a shield will overcome the effects of a magnetic field at frequencies above 1 MHz.

An important effect of magnetic field induction results from the eccentricity of conductors within a cable. In a well-made coaxial cable the central conductor is located in the middle of the dielectric. However, in a poorly made cable and in multiconductor cables, the conductor may be considerably displaced from the centre line of the cable. The effects of this on cable screening can be expressed as an equivalent transfer impedance to a magnetic field. The cancellation of the effects of the field by eddy current is not complete and the presence of holes in a braid constrains the current to take a non-uniform path. This results in an impedance which can be quite significant at low frequencies and may be of the order of 10 mΩ/m in a multiconductor cable.

3.4 Sample of Electromagnetic Interference (EMI)

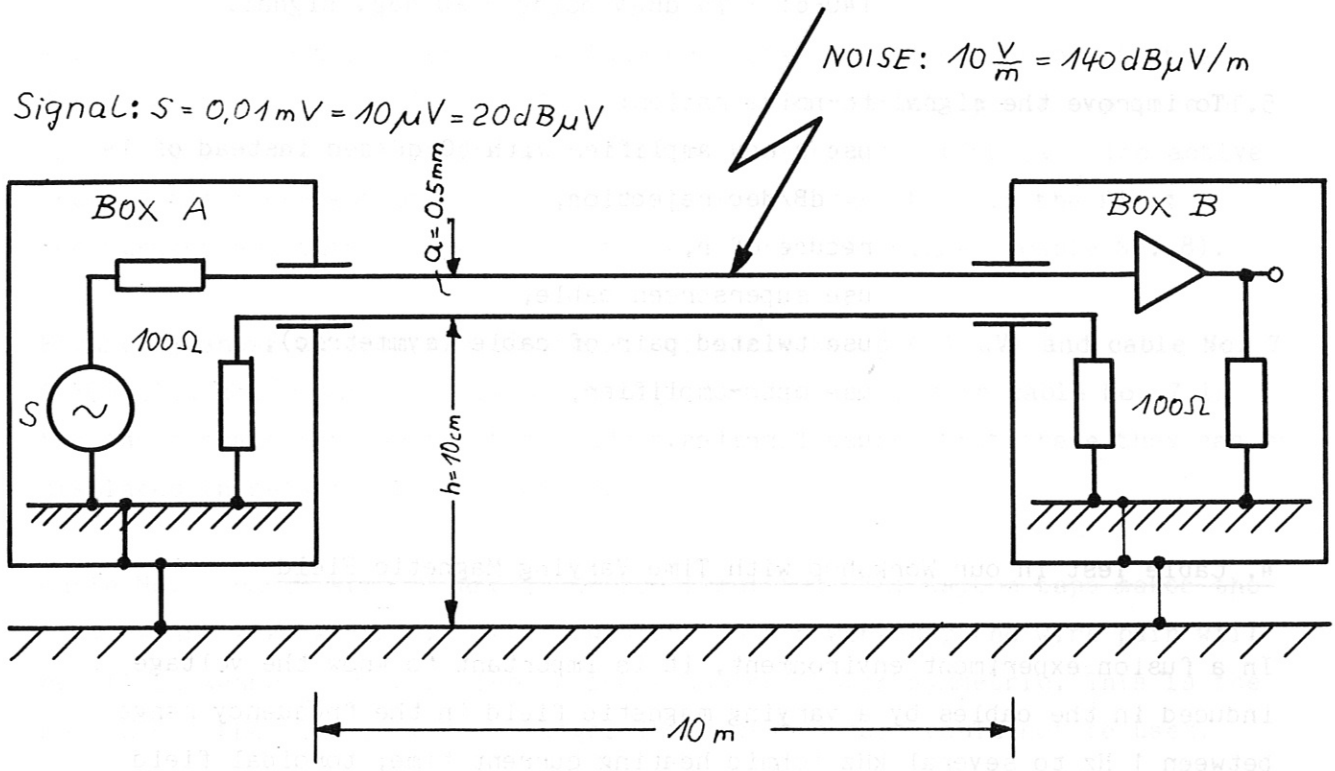

2 ≙	3 dB	Amplifier:
2 ≙	6 dB	
3 ≙	10 dB	bandwidth: 200 kHz
10 ≙	20 dB	filter: 20 dB/dec
100 ≙	40 dB	rejection: 14 dB
1000 ≙	60 dB	

1. Signal 20 dBµV

2. Noise (EMI) 140 dBµV/m

3. This noise is reduced by:

14 dB	amplifier rejection,	*
40 dB	common-mode coupling,	*
7 dB	ground loop coupling.	*
∑61 dB		

* see tables of DON WHITE, Gainesville, Virginia, USA

4. The noise level is still higher than the signal:

140-61 = 79 dBμV noise > 20 dBμV signal.

5. To improve the signal-to-noise ratios:

use a new amplifier with 60 dB/dec instead of 14 dB/dec rejection,
reduce of h,
use superscreen cable,
use twisted pair of cable (symmetric),
use opto-amplifier,
use ferrites.

4. Cable Test in our Workshop with Time Varying Magnetic Field

In a fusion experiment environment, it is important to know the voltage induced in the cables by a varying magnetic field in the frequency range between 1 Hz to several kHz (ohmic heating current time; toroidal field current rise time; vertical field current rise time; plasma disruptions). Computer programs of the magnetic field lines have shown that the largest magnetic field gradient in ASDEX is about 28 mT (280 G) per cm length.

We simulated this field gradient in our workshop with two coils and a current of 20 A. The test set-up is shown in Figs. 14 and 15. No. 1 in Figure 15 shows the test coil with an iron yoke. No. 2 is the tested cable - in this case a twisted pair. No. 3 shows an electrical motor to move the cable through the magnetic field lines. At No. 4 on the cable we soldered a short circuit and at No. 5 we connected the cable to a differential amplifier at an oscilloscope. The magnetic field gradient at the set-up is shown in Fig. 16. The maximal field gradient is 20 mT (200 G) per cm which is in the range of the field gradient in ASDEX. Figures 17 and 18 show examples of the tested cables. The maximal induced voltage is given in Figures 20 to 22 for a current change of 1 s and shown above the cable number in Fig. 17.

More information about the individual cable is listed in Fig. 19. The oscillograms of the induced voltages are listed below:

Cable No.	Fig. No.
1	20
6	23
7	23
8	21/22

Figure 20 shows the induced voltage in cable No. 1 which is a coaxial cable.

Figure 21, cable No. 2, shows the induced voltage of a quard cable in the first twisted pair (2 μV), and Figure 22 the induced voltage in one wire of the first and one wire of the second twisted pair cable (200 μV). The active area of the last-mentioned arrangement is much larger than in the first arrangement and this is the reason for the very high signal (cable No. 8).

Figure 23 shows an enlarged photograph of cable No. 6 (~1 μV) and cable No. 7 (1500 μV). The reason for the very large induced voltage in cable No. 7 is the large space between the two conductors and the fact that these they can be displaced in relation to each other.

Cable No. 7 has 7 strands and is Kapton-insulated. The Kapton tape makes the Cu wire act like a spring. After twisting in our workshop the wire pair will recoil backwards and each wire is loose and no longer symmetric. This is the reason for the high induced voltage. This twisted pair could not be used.

The test with changing magnetic field shows that:

1.) A voltage can be induced even in symmetric coaxial cable when the magnetic field gradient is high enough.
2.) To reduce this effect, only a magnetic shield with highly permeable material is useful (no saturation).
3.) The behaviour of a twisted cable in a varying magnetic field is good even without magnetic shielding material.

Transmitted frequency for

a) coaxial cable: several hundred MHz
b) twisted cable: ≦ 500 kHz

The capacitance per metre of a twisted pair is much larger than that of a coaxial cable. At frequencies above 500 kHz, the signal amplitude decays at lengths greater than 30 m.

5. Induced Voltage in Cables Measured in ASDEX during a 30 kA Ohmic Heating Pulse

To prove our test results described in Sect. 4, we mounted 3 cables close to the ohmic heating coils (distance about 2 cm). We soldered a resistor at the cable end which has the same resistance as the cable impedance. At the other end of the cable we measured the induced voltage during the firing of the zero injection bank of the ohmic heating circuit with an oscilloscope. The total cable length of each cable was 30 m. The induced voltage is listed in the following table:

Table 1

Current change [kA]	Time (ms)	Induced voltage in the cable [mV]	Type of cable	Cable outside diameter [mm]	Cable attenuation at 10 MHz [dB per 100 m]	Price [DM per metre]
1.4	1	1.5	Coaxial 50Ω; RG58C/U (Cable No. 1 in Sect. 4)	5	4.8	~ 0.80
1.4	1	3.0	Twin cable 78Ω; RG108A (Cable No. 2 in Sect. 4)	6+	4.5	~ 1.80
1.4	1	0.3	Twisted pairs; AWG 24 (Cable No. 4 in Sec. 4)	3.5	5.3*	~ 4.00

\+ not acceptable for Lemosa connectors, size 0 ($\leq$ 4.2 mm)

* twisted pair cable should be used only up to frequencies of 500 kHz (30 m)

6. Twisted Pair Cable

Figure 24 shows the coupling rejection versus the number of twists per metre cable length. This calculation was made according to the course notebook for electromagnetic compatibility presented by Don White, Gainesville, Virginia, U.S.A.

7. Calculation of a Double Magnetic Shell and its Efficiency as a Magnetic Shield for a Coaxial Cable with 12 Conductors against External Magnetic Fields

A rigid steel-iron conduit has excellent shielding properties, even better than those of a solid copper pipe of equivalent size. The permeability of the steel more than offsets the higher resistivity of the steel. But this performance can only be obtained if the high-permeability material is not in saturation. The following cable (see Fig. 25) is calculated for a stray field in air of $B < 20 \left[\text{mT}\right]$. Above this level the shielding efficiency will be reduced.

$B_1 = 20 \left[\text{mT}\right]$ MAGNETIC INDUCTION IN AIR CREATED BY POLOIDAL MAGNETIC FIELD COILS AND THE PLASMA CURRENT. NOTE THE MAGNETIC FIELD GRADIENT OF ABOUT $20\left[\text{mT}\right]$ per $\left[\text{cm}\right]$ LENGTH IN THE ENVIRONMENT OF A TOKAMAK.

B_2 MAGNETIC INDUCTION IN THE MATERIAL CALLED PERMENORM WITH SATURATION INDUCTION $B_{2S} = 1.35 \left[\text{T}\right]$; PERMEABILITY $\mu_{2A} = 3{,}000 \left[1\right]$ and $\mu_{2max} = 35{,}000 \left[1\right]$.

B_3 MAGNETIC INDUCTION BETWEEN THE TWO DIFFERENT IRON LAYERS.

B_4 MAGNETIC INDUCTION IN THE MATERIAL CALLED MU-METAL.

B_5 MAGNETIC INDUCTION INSIDE THE TWO SHELLS WHERE THE 12 COAXIAL CABLES ARE.

B_{4S} $= 0.8\left[\text{T}\right]$ SATURATION INDUCTION; PERMEABILITY (mu-metal) $\mu_{4A} = 25{,}000\left[1\right]$ and $\mu_{4max} = 80{,}000\left[1\right]$

N.B. CABLE FACTORY: Felten + Guilleaume; W. Germany
PRICE PER METRE: DM 40.-- (1979)

1. MAGNETIC FLUX

$$\Phi_{Fe} = \Phi_{air} = B_{Fe} \cdot A_{Fe} = B_{air} \cdot A_{air}$$

D = SHELL DIAMETER [mm]

area: $A_{air} = D \cdot l$

l = CABLE LENGTH [m]

$$A_{Fe} = 2 \cdot t \cdot l$$

t = SHELL THICKNESS [mm]

2. SHIELDING EFFICIENCY OF THE FIRST (OUTER) IRON SHELL (PERMENORM)

$$\Phi_{Fe} = \Phi_{air} = B_{2(Fe)} \cdot A_2 = B_{1(air)} \cdot A_1 \quad ; \quad B_2 \cdot 2 \cdot t_2 \cdot l = B_1 \cdot D_2 \cdot l$$

$$B_2 = B_1 \cdot \frac{D_2}{2 \cdot t_2} = \frac{20[\text{mT}] \cdot 22[\text{mm}]}{2 \cdot 0.2[\text{mm}]} \quad ; \quad \underline{\underline{B_2 = 1.1[\text{T}] < B_{2S} = 1.35[\text{T}]}} \quad \text{O.K.}$$

2.1 SHIELDING FACTOR

$$S_2 = \frac{B_1}{B_3} = \frac{\mu_{2A} \cdot t_2}{D_2} + 1 = \frac{3000 \cdot 0.2[\text{mm}]}{22[\text{mm}]} + 1 \quad ; \quad \underline{\underline{S_2 = 28[1]}}$$

$$S_2' = 20 \log (S_2) = 20 \cdot \log (28) \qquad S_2' = 29[\text{dB}]$$

$$B_3 = \frac{B_1}{S_2} = \frac{20[\text{mT}]}{28} \qquad B_3 = 0.72[\text{mT}]$$

3. SHIELDING EFFICIENCY OF THE SECOND (INNER) IRON SHELL (MU-METAL)

$$\Phi_{4(Fe)} = \Phi_3 = B_{4(Fe)} \cdot A_4 = B_3 \cdot A_3 \; ; \; B_4 \cdot 2 \cdot t_4 \cdot 1 = B_3 \cdot D_4 \cdot 1$$

$$B_4 = B_3 \frac{D_4}{2 \cdot t_4} = \frac{0.72\left[\text{mT}\right] \cdot 21.2\left[\text{mm}\right]}{2 \cdot 0.2\left[\text{mm}\right]} \; ; \; \underline{\underline{B_4 = 38\left[\text{mT}\right] < B_{4S} = 800\left[\text{mT}\right]}}$$

3.1 SHIELDING FACTOR

$$S_4 = \frac{B_3}{B_5} = \frac{\mu_{4A} \cdot t_4}{D_4} + 1 = \frac{25000 \cdot 0.2\left[\text{mm}\right]}{21.2\left[\text{mm}\right]} + 1 \; ; \quad \underline{\underline{S_4 = 236\left[1\right]}}$$

$$S_4' = 20 \log (S_4) = 20 \cdot \log (236) \qquad S_4' = 47\left[\text{dB}\right]$$

4. TOTAL SHIELDING FACTOR (FOR TWO SHELLS)

$$S \approx S_2 \cdot S_4 \cdot 4 \cdot \frac{\Delta}{D_2} = 28 \cdot 236 \cdot 4 \cdot \frac{0.2\left[\text{mm}\right]}{22\left[\text{mm}\right]} \; ; \; \underline{\underline{S = 242\left[1\right]}}$$

$$S' = 20 \log (S) = 20 \log (242) \qquad S' = 48\left[\text{dB}\right]$$

$$B_5 = \frac{B_1}{S} = \frac{20\left[\text{mT}\right]}{242} \qquad B_5 = 0.082\left[\text{mT}\right]$$

8. Shielding

Good shielding efficiency for (high-impedance) electric fields is obtained by using high-conductivity materials such as copper /6/.

The High-permeability materials (mu-metal: μ_r = 80,000) are interesting for their low-frequency, magnetic field shielding properties /7/. However, they are prone to saturation at low field densities and require careful handling procedures. Figure 26 shows the shielding efficiency of a 0.25 mm thick copper and mu-metal shield as a function of frequency.

9. Common-mode Impedance Coupling

The development of the common mode voltage (CMV) is shown in Fig. 27 /8/. The current J(t) creates a magnetic field B varying with time in the area of the electric circuit. This induced voltage between the circuit and the ground plane is called the common-mode voltage ($U_{2,3}$). The amplifier, connected with conductors 1 and 2, must have a common-mode rejection higher than the common-mode voltage which is created by the current J(t) /9/.

The induced voltage created at points 1 and 2 is called the differential-mode voltage (U_{DMV}). The area $A_{1,2}$ is relatively large and therefore the signal $U_{1,2}$ is high. To reduce these voltages, one should reduce the area $A_{1,2}$. The lower part of Fig. 27 shows a pair of twisted cables (connected at points I and II). If the sum of the areas Aa and Ab are equal, the differential-mode voltage is $U_{DMV} \rightarrow 0$ /10/.

Figure 28 shows the three sources of common-mode noise /11/.

10. Special Cable Arrangements for High Temperatures and High-vacuum Conditions

In order to keep evaporation of the cable insulation inside the vacuum vessel as small as possible, we used two different cable arrangements, e.g. for the Mirnov probes. In Fig. 29 one can see a pair of twisted Teflon-insulated wires inside a secondary tube system, connected to a feed-through and to the Mirnov coil (magnetic probe). By pumping, we got an intermediate vacuum inside the tube. Even with small leaks of the feed-through, the high-vacuum system is hardly affected. The temperature of this arrangement is limited to 260 °C (Teflon insulation). This system is reliable but complicated.

A second arrangment of a cable system for Mirnov probes is shown in Fig. 30. A magnetic probe made of mineral-insulated cable is shown in Fig. 30, position 1. The insulation of this cable is magnesium oxide (MgO), which is hygroscopic. This material tends to collect moisture from the air. To prevent this behaviour, we designed a thermal box. With a tube 4 mm in diameter, we can exhaust this thermal box so that the magnesium oxide is not exposed to moisture. Inside the box, the coaxial cables are connected to a two-conductor mineral-insulated cable. The connection is made by crimping the Inconel conductors. We tested the system with a voltage of 0.5 kV between the conductor and vacuum vessel wall. This cable arrangement is very reliable up to about 1000°C.

11. Example of an Electric Circuit in an Experiment Environment

A frequency-selective grounding technique is used to transmit a signal from a tokamak diagnostic to an amplifier at a distance of several tenths of a meter.

For low frequencies single-point grounding is required (see point A in Fig. 31). For high (RF) frequencies multiple-point grounding is required. In Fig. 31 one can see an additional capacitive grounding on the cable shield at point C. This grounding point reduces standing waves which could be created by Alfven wave or ion cyclotron heating. It is highly recommended that the circuitry be made accessible for testing by opening the switch at point B. The circuit should then not be grounded at all (for DC voltage test). To reduce the noise created in the circuit a small source impedance (e.g. z_g = 100 ohm) should be used. The common-mode rejection is calculated by the equation

$$CMR = 20 \cdot \log_{10} \frac{U_i}{U_o} \left[dB \right] ,$$

where U_i is the common-mode voltage and U_o the differential-mode voltage (see Fig. 31).

12. Noise Reduction

As power systems grow (neutral injection, ion cyclotron resonance and lower hybrid resonance heating) new levels of noise are created. The thyristor voltage spikes of the rectifiers for the poloidal and toroidal power supplies are of real concern.

The large structural dimensions of a tokamak system become important when transient phenomena occur. The low-resistance grounding grid cannot be considered to be a unipotential surface because the inductance becomes so large at the transient frequencies. In this environment, control and diagnostic cables become quite long. The magnetic fields and the electrostatic field strength are very high. The cables are exposed to capacitive or electrostatic coupling and to actual potential differences. Tokamak diagnostic measurements in this environment superimpose electric noise on the measured signal. If not controlled, the noise can lead to inaccurate results and incorrect interpretation of the control and diagnostic signals.

Some rules for reducing the noise in the cabling system are as follows:

1. Wiring

Use a radial run of all wiring from the experiment to the diagnostic panels. The remote ends of the cables should not be interconnected with any other circuitry. Cable loops must be avoided and a tree-shaped grouping of the cable branches be used. One cable end (the cable end with the lowest impedance) should be grounded and the other cable end terminated by a capacitor to reduce standing waves on the cable shield (avoid ground loops). The capacitance should be of the order of 0.1 μF.

2. Cable sheath

The metallic cable sheath should have the lowest possible impedance. A shield made of ferrous material can only be used if the saturation flux of the material is higher than the magnetic flux in the air in which the cable is located.

3. Cable length

The control cables should be as short as possible and oriented at right angles to the primary bus bars.

4. Damping resistors

The transient oscillation between circuitries could be damped by a low resistance at each pole of the control cable. The resistance value for critical damping for a typical installation should be about 100 ohm.

5. Electrostatic noise

Alternating electric fields inject noise into the cable system through the phenomenon of capacitve coupling (see Fig. 7). To reduce this noise, the distance between the cable and electrostatic source has to be increased and the cable diameter has to be made as small as possible (to decrease the stray capacitance C_s).

6. Electromagnetic noise

Use a cable with a pair of twisted conductors. If the twisting is symmetric and the field gradient per twist small, then the induced voltage per twist is cancelled out. We used a cable with 2 conductors. The size at the leads is AWG 24 (0.25 mm^2 Cu) and one twist per 6 mm cable length.

In an environment with high magnetic field gradients the induced voltage of a coaxial cable will not be completely cancelled. For this type of cable a permenorm and a mu-metal shield with high permeability are necessary (to obtain saturation).

7. Ground connection

All conductors are characterized by resistance, inductance and shunt capacitance. As a result, attention should always be given to the quality of the ground wire. An effective ground connection should be made of heavy-gage insulated copper wire as short as possible.

13. Typical Damage Energies of Electronic Components

Device Type	Energy μWs
Microwave diode	0.1
Integrated circuits	10.0
Low-power transistors	20 ÷ 1000
High-power transistors	1000
Zener diodes	1000
Rectifiers	500
Resistors (0.25 W)	10^4
Relays	10^5
Transformer	10^9

14. Overvoltage Protection

Until recently it was widely believed that a gas-filled arrestor alone was too slow for striking voltages with high growth rates. Industry have now designed a surge arrestor with the following data:

1. Type: 112/230 GEC with copper wire termination

Size: diameter: 8 mm
length: 6 mm

Characteristics:

DC striking voltage	$195 \div 265 \left[V\right]$
* Surge striking voltage	$400 \left[V\right]$
Insulation resistance at 170 VDC	$10^9 \left[Ohm\right]$
Capacitance	$2.5 \left[pF\right]$
Max peak current	$10 \left[kA\right]$
Destruction current	$I_{rms} = 15 \left[A\right]; \; t = 1 \left[s\right]$

Gap-gap transfer time	8 [µs]
Price	approx. 3,-- DM/each

* measured on a 1 kV/µs rising voltage ramp

2. Type: 49A M-O Valve Company

Characteristics:

DC striking voltage	210 ÷ 310 [V]
* Surge striking voltage	700 [V]
Insulation resistance at 100 VDC	10^{10} [Ohm]
Max peak current	5 [kA]
Gap-gap transfer time	0.1 [µsec]
Price	approx. 12,-- DM/each

Safeguards

Comparing the coupled-in spurious signals with the interference or damage thresholds of the electronic components shows the great danger to electrical equipment and systems.

To prevent coupling of the high voltage input via signal and power supply lines, one can use:

charge arrestors (limitation of the amplitude),
filters (limitation of the bandwidth),
cable shielding,
proper grounding concept (avoid ground loops),
if possible, cable with twisted pairs.

The sum of all safeguards must be dimensioned to ensure adequate decoupling between the spurious voltage signals and the susceptibility of the electronics.

Figure 32 shows an example of an electromagnetic compatibility (EMC) circuit protecting the electronic components.

15. Appendix A: Decibels

It is usual to measure the voltage or power ratios in electromagnetic interference problems in decibels [dB]:

$$\text{voltage ratio:} \quad U = 20 \log_{10} \frac{U_2[V]}{U_1[V]} [dB],$$

$$\text{power ratio:} \quad P = 10 \log_{10} \frac{P_2[W]}{P_1[W]} [dB].$$

A calculation in decibels reduces multiplication into a much simpler addition, e.g.

$$20\ dB + 40\ dB = 60\ dB \mathrel{\hat{=}} 1000,$$

$$10 \times 100 = 1000$$

Factor	Power ratio [dB]	Voltage ratio [dB]
1.4	1.5	3
2	3	6
3	5	10
5	7	14
10	10	20
100	20	40
1000	30	60

Power ratio:

$$0\ dB \mathrel{\hat{=}} 10^{0} \mathrel{\hat{=}} 1$$
$$1\ dB \mathrel{\hat{=}} 10^{0.1} \mathrel{\hat{=}} 1.259$$
$$3\ dB \mathrel{\hat{=}} 10^{0.3} \mathrel{\hat{=}} 2$$
$$10\ dB \mathrel{\hat{=}} 10^{1} \mathrel{\hat{=}} 10$$
$$20\ dB \mathrel{\hat{=}} 10^{2} \mathrel{\hat{=}} 100$$
$$30\ dB \mathrel{\hat{=}} 10^{3} \mathrel{\hat{=}} 1000$$

Signal levels can be expressed in for example, mV or dBmV (decibels above one millivolt). They may be identified in the following relations:

$$U\left[dBmV\right] = +\ 20\ \log_{10}\left(U\left[mV\right]\right)$$
$$+\ 60\left[dB\right] + U\left[dB\mu V\right] \qquad \left(60\ dB \mathrel{\hat{=}} 1000 = \frac{U\left[mV\right]}{U\left[\mu V\right]}\right)$$
$$+\ 60\left[dB\right] + J\left[dB\mu A\right] + 20\ \log_{10}\left(Rg\left[\Omega\right]\right)$$
$$-\ 60\left[dB\right] + J\left[dB\mu A\right] + 20\ \log_{10}\left(Rg\left[\Omega\right]\right)$$
$$-\ 13\left[dB\right] + P\left[dBm\right] \quad \text{for } Rg = 50\,\Omega \text{ source resistance} \qquad 1.)$$

dBV $\mathrel{\hat{=}}$ dB above 1 V
dBμV $\mathrel{\hat{=}}$ dB above 1 mV
dBA $\mathrel{\hat{=}}$ dB above 1 A
dBμA $\mathrel{\hat{=}}$ dB above 1 mA

dBm(W) $\mathrel{\hat{=}}$ dB above 1 mW

J $\mathrel{\hat{=}}$ signal source current in amperes
U $\mathrel{\hat{=}}$ signal source voltage in volts
Rg $\mathrel{\hat{=}}$ signal source resistance in ohms
P $\mathrel{\hat{=}}$ signal source power in watts
NdBmV $\mathrel{\hat{=}}$ sensitivity (noise level) in dBmV for analog systems
NdBmV $\mathrel{\hat{=}}$ noise immunity level (NIL) in dBmV for digital systems

$$P = \frac{U^2}{Rg}$$

$$U^2 = Rg \cdot P$$

$$U = \sqrt[2]{Rg \cdot P}$$ change to logarithmic equation

$$\log(U) = 1/2 \log(Rg) + 1/2 \log(P)$$

$$20 \log(U) = 20/2 \log(Rg) + 20/2 \log(P) \text{ ; (multiplied by factor of 20)}$$

$$20 \log(U) = 10 \log(Rg) + 10 \log(P)$$

$$U\left[dB\right] = 20 \log_{10} \frac{U_2\left[V\right]}{U_1\left[V\right]} \left[1\right]$$

$$U\left[dB\right] = 10 \log_{10} \frac{P_2\left[W\right]}{P_1\left[W\right]} \left[1\right]$$

$$U\left[dBV\right] = 10 \log (Rg\left[\Omega\right]) + P\left[dB\right] \quad \text{(Watts)}$$

$$60\left[dB\right] + U\left[dBmV\right] = 10 \log (Rg\left[\Omega\right]) + 30\ dB + P\left[dBm\right] \quad \text{(milli-Watts)}$$

$$U\left[dBmV\right] = -30dB + 10 \log (Rg\left[\Omega\right]) + P\left[dBm\right] \text{ ; for } Rg = 50\left[\Omega\right]$$

$$\log(Rg) = \log(50) = 1.7 \left[1\right]$$

$$10 \log(50) = 17\left[dB\right]$$

$$U\left[dBmV\right] = -13\left[dB\right] + P\left[dBm\right] \text{ ; for } Rg = 50\left[\Omega\right]$$

16. Appendix B: Insulation Material for Cables

Figure 33 shows the insulation material for cables which could be used in TOKAMAK environment.

17. Appendix C: a New Special Cable for High-vacuum Conditions

The upper part of Fig. 34 shows a glass-silk-insulated and twisted cable with stainless-steel conductor (0.5 mm diameter) and stainless-steel screen. This cable will be used for the Mirnov coil connection inside the vacuum vessel to the feed-through (cable type SK 2L-E; see Fig. 35).

The lower part of Fig. 34 shows a glass-silk-insulated cable for thermocouples. One end has a glass bead melted on.

Figure 36 makes general remarks and gives the order codes /12/.

Acknowledgements:

H.J. Berger is thanked for testing several different kinds of cables in the workshop. The author is also grateful to T. Henningsen for preparing the photographs and G. Janowski for writing the text.

Note:

Reference to a company product or name does not imply approval or recommendation of the product by IPP to the exclusion of others that may be equally suitable.

18. References

/1/ Gernhardt, J., et al., IPP Report III/65 (1981)
An Equipment Protection and Safety System for ASDEX Tokamak.
See Fig. 39 for notations.

/2/ DON WHITE
Gainesville, Virginia, U.S.A.

/3/ Vishay, Raleigh
Tech Note TN-501
Noise Control in Strain Gage Measurements,
North Carolina, U.S.A.

/4/ Verein Deutscher Ingenieure, Verband Deutscher Elektrotechniker (VDI/VDE)
Empfehlungen zur Störsicherheit der analogen Signalübertragung beim Einsatz von Prozeßrechnern,
VDI/VDE 3551, June 1975.

/5/ M. Green
Optimized and Supersreened Cables,
Raychem.

/6/ D.R.J. White
EMC Handbook Vol. 3,
Germantown, Maryland, U.S.A.

/7/ Vakuumschmelze D-6450 Hanau
Magnetische Abschirmungen,
FS-M9/1975.

/8/ Electromagnetic Interference Control in Industrial Facilities,
EMC Technology, January 1982.

/9/ H.C. Ramberg
Methods for Reducing Induced Voltages in Secondary Circuits,
IEEE Transactions on Power Apparatus and Systems,
Vol. Pos. 86, No.7, July 1967, p. 907-912.

/10/ D. Stoll
EMC Elektromagnetische Verträglichkeit (Electro Magnetic Compatibility)
Elitera-Verlag, Berlin 33, DK 621.391.82:62-758.37/.38.

/11/ Physikalisch-Technische Bundesanstalt
Störspannungen und Störströme auf Leitungen. Meßverfahren und Meßergebnisse.
PTB-Bericht E-15, August 1980, ISSN 0341-6674.

/12/ Sulzer Brothers Ltd. Nuclear Engineering Division,
CH-8401 Winterthur, Switzerland.

19. Figure Captions

Fig. 1 Coupling of noise X_Z into the measured signal X_D

Fig. 2 Example of an electric circuit with simple cable model

Fig. 3 A two-box equipment EMI situation with 500,000,000 combinations

Fig. 4 High-impedance, electric-field source and wave

Fig. 5 Low-impedance, magnetic-field source and wave

Fig. 6 Wave impedance as a function of source distance

Fig. 7 Electrostatic noise coupling (capacitive coupling)

Fig. 8 Electromagnetic noise coupling (inductive coupling)

Fig. 9 Electrostatic shielding (Faraday Cage)

Fig. 10 Cross-section of a hollow rectangular solid of high permeability immersed in a uniform magnetic field showing distribution of magnetic field lines

Fig. 11 Coupling rejection as a function of frequency f by capacitive coupling

Fig. 12 Variation of the surface transfer impedance with frequency f for different cable screen constructions

Fig. 13 Coupling rejection as a function of frequency f by magnetic coupling

Fig. 14 Schematics of cable test arrangement in our workshop

Fig. 15 Cable test arrangement in our workshop

Fig. 16 Magnetic field gradient as a function of distance of our test magnet

Fig. 17 Different kinds of tested cables and the value of the measured induced kinds of tested cables and the value of the measured induced voltage U[µV] in our test arrangement

Fig. 18 Cable and magnetic shielding arrangements

Fig. 19 List of different cable types

Fig. 20 Oscillogram of a tested coaxial cable type RG 58C/U

Fig. 21 Oscillogram of a tested Teflon cable with pairs of twisted conductors size AWG 24 (one twist per 5 mm of cable length)

Fig. 22 Oscillogram of a tested 4-conductor cable with 2 twisted pairs

Fig. 23 The upper part of the picture shows a pair of twisted cables with Teflon insulation. The lower part shows a pair of twisted cables with Kapton insulation

Fig. 24 Coupling rejection offered by twisting wire pair

Fig. 25 Magnetic shield for 12 coaxial cables

Fig. 26.0 Shielding effectiveness of copper versus frequency

Fig. 26.1 Shieling effectiveness of iron versus frequency

Fig. 26.2 Shielding effectiveness of material with high permeability versus frequency

Fig. 27 Development of common mode voltage U_{CMV} and differental mode voltage U_{DMV}

Fig. 28 Three sources of common-mode noise

Fig. 29 Magnetic probe with feed-through and wiring

Fig. 30 Magnetic probe connected with mineral-insulated cables (MgO)

Fig. 31 Example of an electric circuit in an experimental environment

Fig. 32 Electronic circuit protected by surge arrestors against spurious voltage signals

Fig. 33 Insulation material for cables

Fig. 34 Pair of twisted cables with glass silk insulation

Fig. 35 Specification for silk-insulated cables

Fig. 36 General remarks and order code

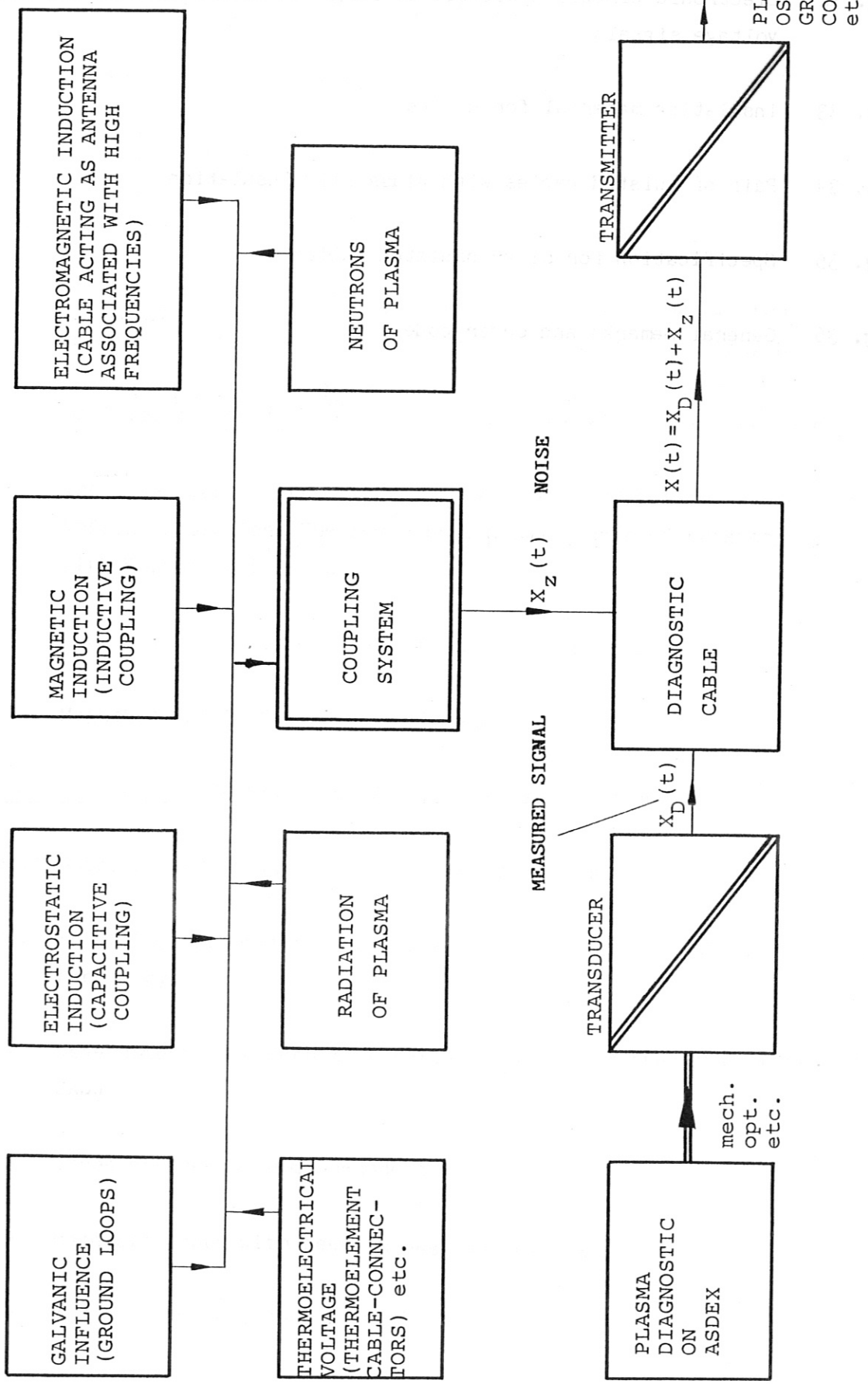

FIG.: 1 COUPLING OF NOISE X_z INTO THE MEASURED SIGNAL (X_D)

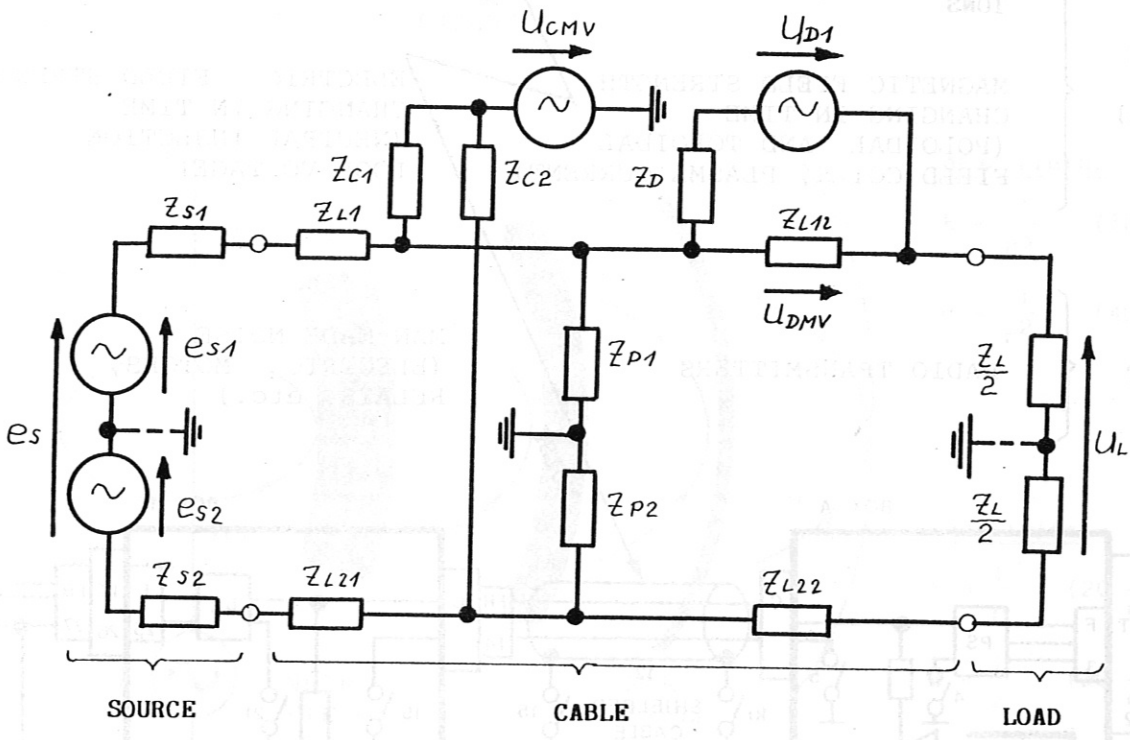

$e_{S(i)}$ [V] ELECTROMAGNETIC FORCE (EMF)

$Z_{S(i)}$ [Ω] SOURCE IMPEDANCE

$Z_{L(i)}$ [Ω] LENGTH IMPEDANCE OF CABLE

$Z_{P(i)}$ [Ω] PARALLEL IMPEDANCE OF CABLE

Z_L [Ω] LOAD IMPEDANCE

U_L [V] LOAD VOLTAGE

$U_{D(i)}$; U_{DMV} [V] DIFFERENTIAL-MODE VOLTAGE

U_{CMV} [V] COMMON-MODE VOLTAGE

Z_D [Ω] COUPLING IMPEDANCE OF DIFFERENTIAL MODE VOLTAGE

$Z_{C(i)}$ [Ω] COUPLING IMPEDANCE OF COMMON MODE VOLTAGE

FIG. 2 EXAMPLE OF AN ELECTRIC CIRCUIT WITH SIMPLE CABLE MODEL

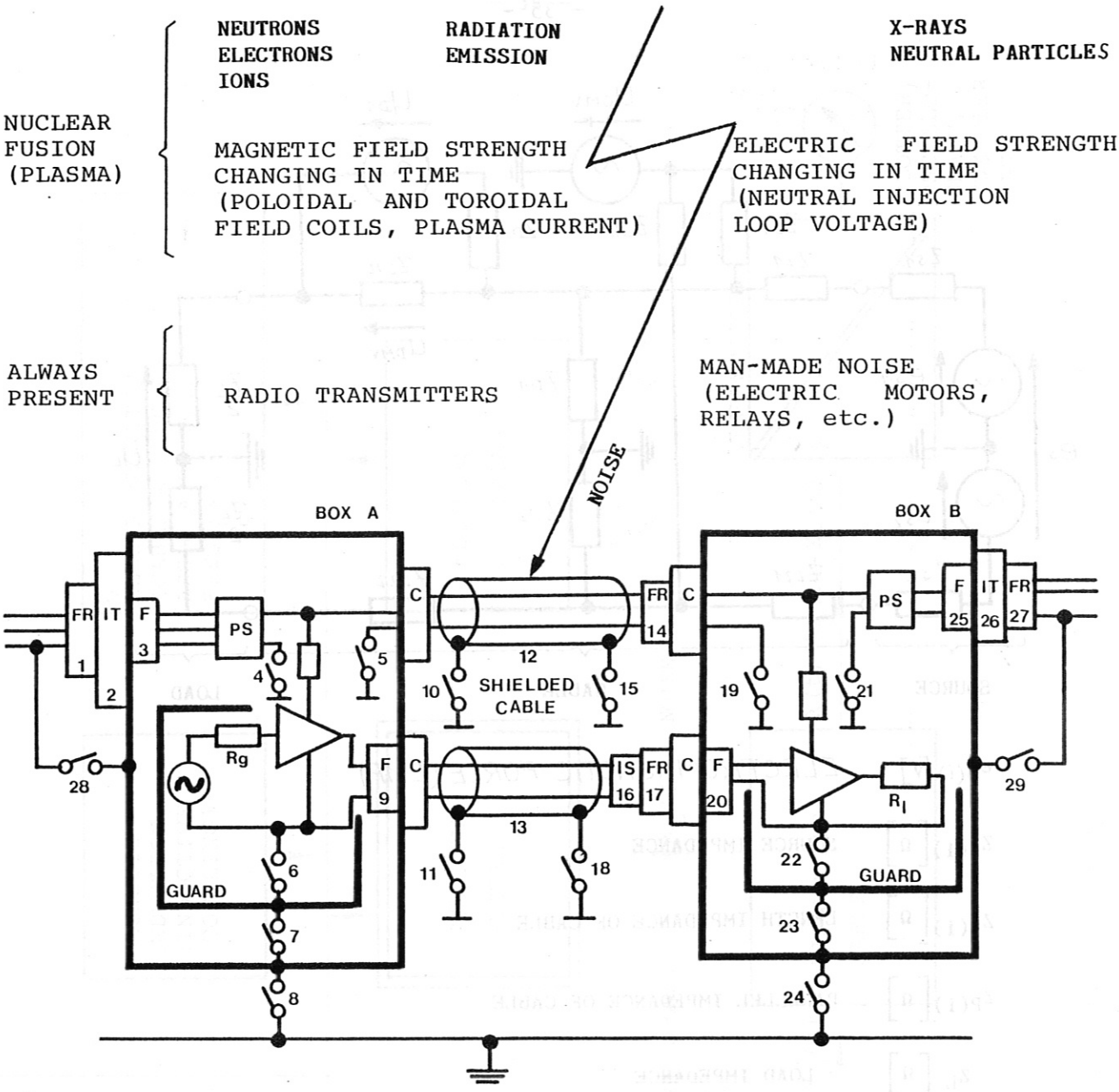

FR FERRITES
IT ISOLATION TRANSFORMER
IS ISOLATORS (OPTICAL OR TRANSFORMERS)
F FILTERS
C CONNECTORS
PS POWER SUPPLY

THE NOS. 1-29 ARE QUESTIONS WITH TWO CHOICES EACH (CLOSED OR OPEN, USED OR NOT USED)

NUMBER OF COMBINATIONS OF THESE 29 QUESTIONS:

$$2^{29} = 500,000,000 \quad \text{POSSIBILITIES}$$

THIS IS THE REASON WHY EMI CONTROL IS SO DIFFICULT.

FIG. 3 A TWO-BOX EQUIPMENT EMI SITUATION WITH 500,000,000 COMBINATIONS

ILLUSTRATION OF FIELD STRENGTH VS. SOURCE TYPE AND DISTANCE

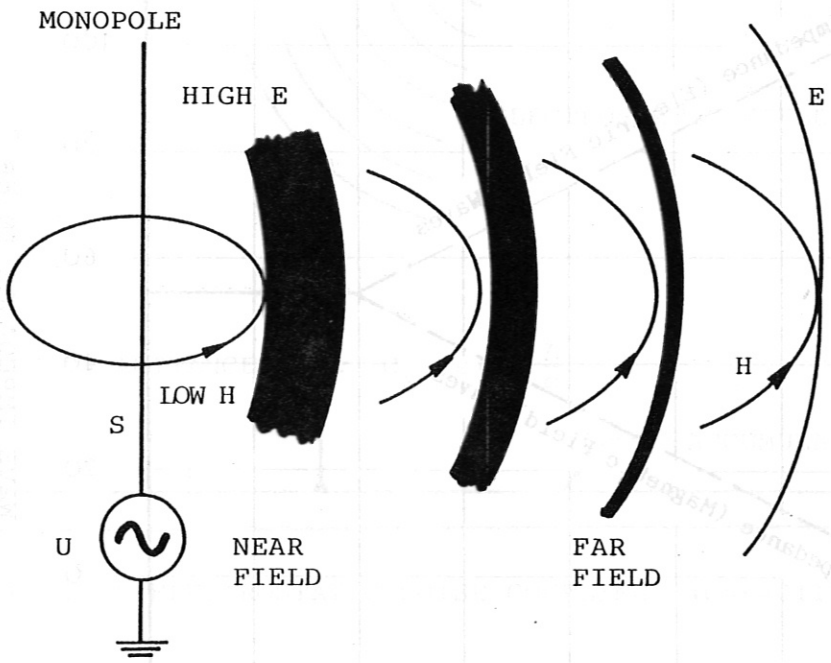

near field:

$E \propto \frac{1}{r^3}$ $(60 \frac{dB}{dec})$

$H \propto \frac{1}{r^2}$ $(40 \frac{dB}{dec})$

far field:

$E \propto \frac{1}{r}$ $(20 \frac{dB}{dec})$

$H \propto \frac{1}{2}$ $(20 \frac{dB}{dec})$

FIG. 4 HIGH-IMPEDANCE, ELECTRIC-FIELD SOURCE AND WAVE

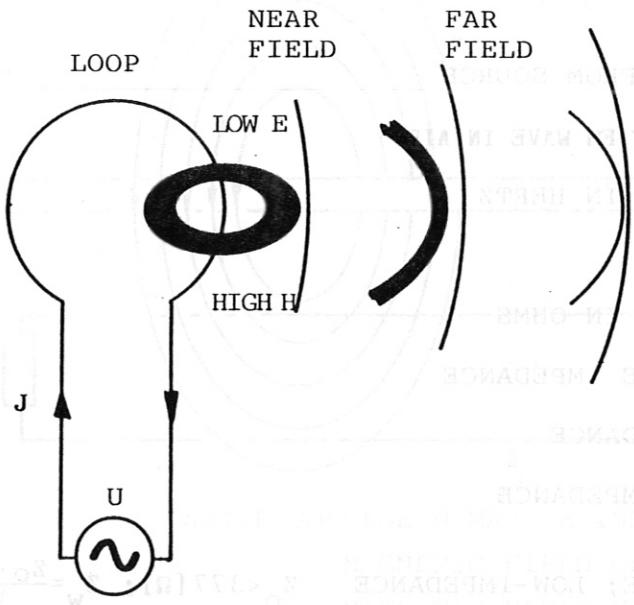

near field:

$E \propto \frac{1}{r^2}$ $(40 \frac{dB}{dec})$

$H \propto \frac{1}{r^3}$ $(60 \frac{dB}{dec})$

far field:

$E \propto \frac{1}{r}$ $(20 \frac{dB}{dec})$

$H \propto \frac{1}{r}$ $(20 \frac{dB}{dec})$

FIG. 5 LOW-IMPEDANCE, MAGNETIC-FIELD SOURCE AND WAVE

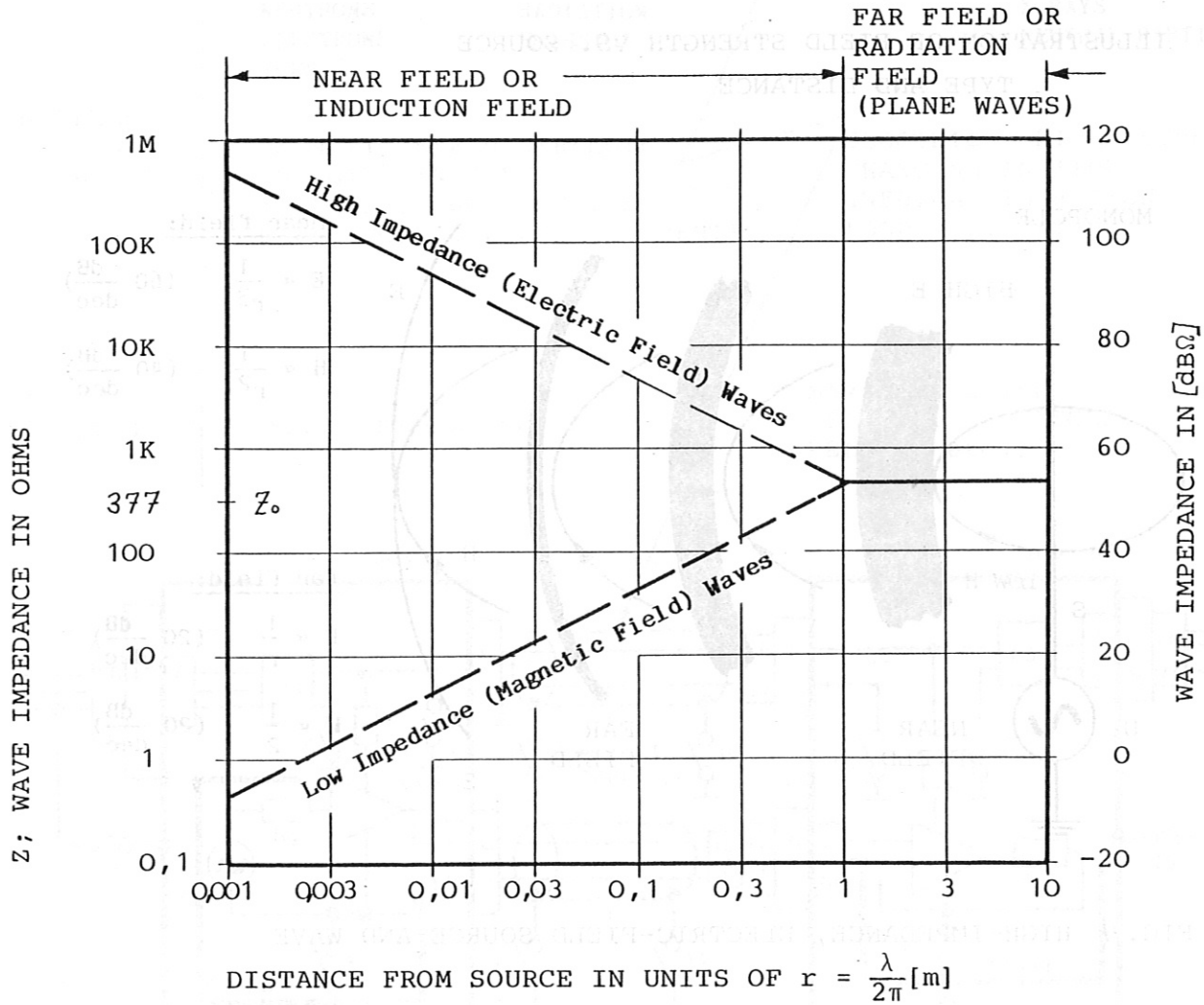

$\lambda = \frac{c}{f}$

r [m]	DISTANCE FROM SOURCE
$c = 3 \cdot 10^8$ [m/s]	**VELOCITY OF EM WAVE IN AIR**
f [Hz]	FREQUENCY IN HERTZ
λ [m]	**WAVELENGTH**
Z [Ω]	IMPEDANCE IN OHMS
$Z_o = 377$ [Ω]	PLANE-WAVE IMPEDANCE
$Z_w = \frac{E}{H}$ [Ω]	WAVE IMPEDANCE
Z_c [Ω]	CIRCUIT IMPEDANCE

1.) MAGNETIC-FIELD WAVE; LOW-IMPEDANCE $Z_o < 377$ [Ω]; $Z_w = \frac{Z_o \cdot 2\pi r}{\lambda} = \frac{E}{H}$
(CONSTANT-VOLTAGE SOURCE)

2.) ELECTRIC-FIELD WAVE; HIGH-IMPEDANCE $Z_o < 377$ [Ω]; $Z_w = \frac{Z_o \cdot \lambda}{2\pi r} = \frac{E}{H}$
(CONSTANT-CURRENT SOURCE)

3.) FAR FIELD (PLANE WAVE); IMPEDANCE $Z_o = 377$ [Ω] AND IS
INDEPENDENT OF THE CIRCUIT SOURCE IMPEDANCE Z_c.

FIG.: 6 WAVE IMPEDANCE AS A FUNCTION OF SOURCE DISTANCE

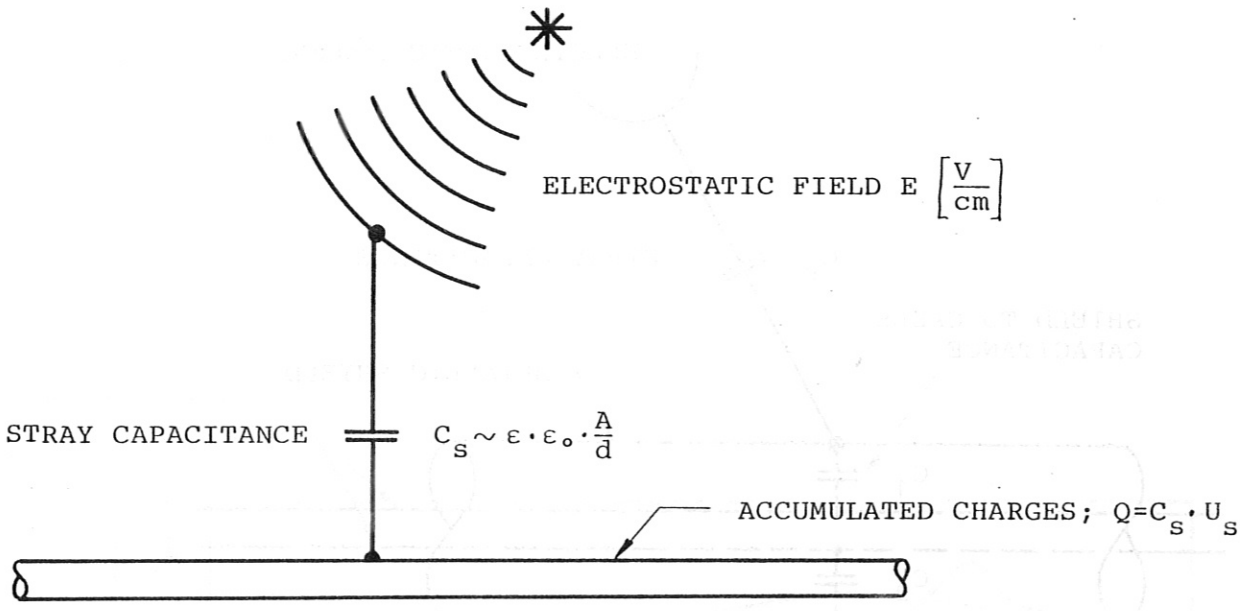

FIG.: 7 ELECTROSTATIC NOISE COUPLING (CAPACITIVE COUPLING)

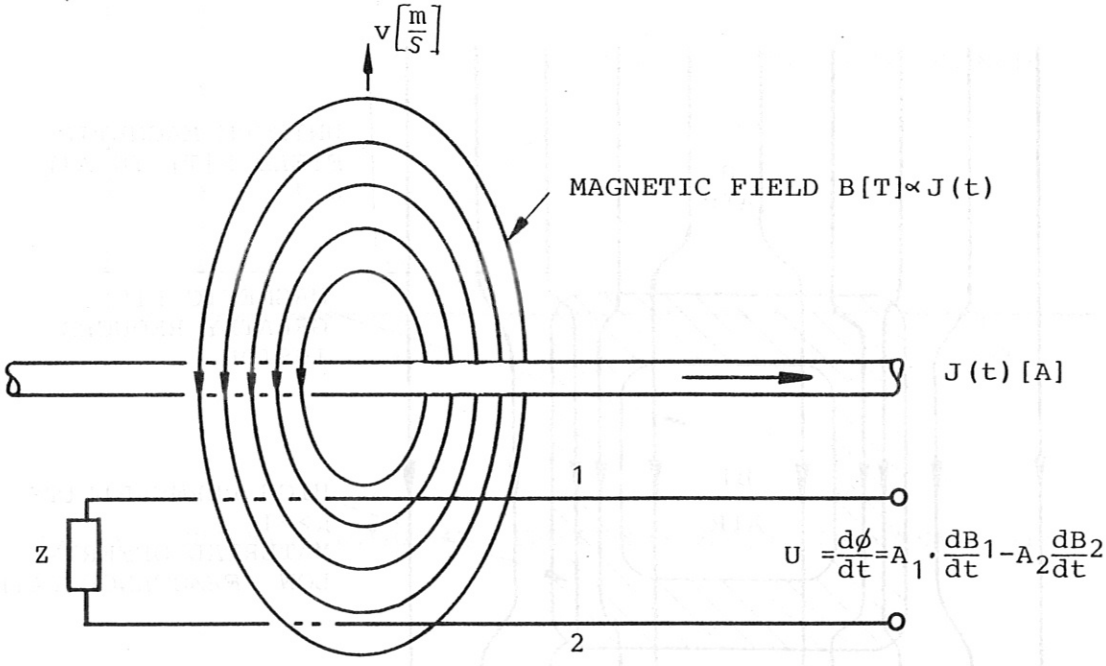

NOISE VOLTAGE U MAY BE INDUCED BY

1) MAGNETIC FIELD CHANGES DURING TIME OR
2) MAGNETIC FIELD MOVES WITH VELOCITY v

FIG.: 8 ELECTROMAGNETIC NOISE COUPLING (INDUCTIVE COUPLING)

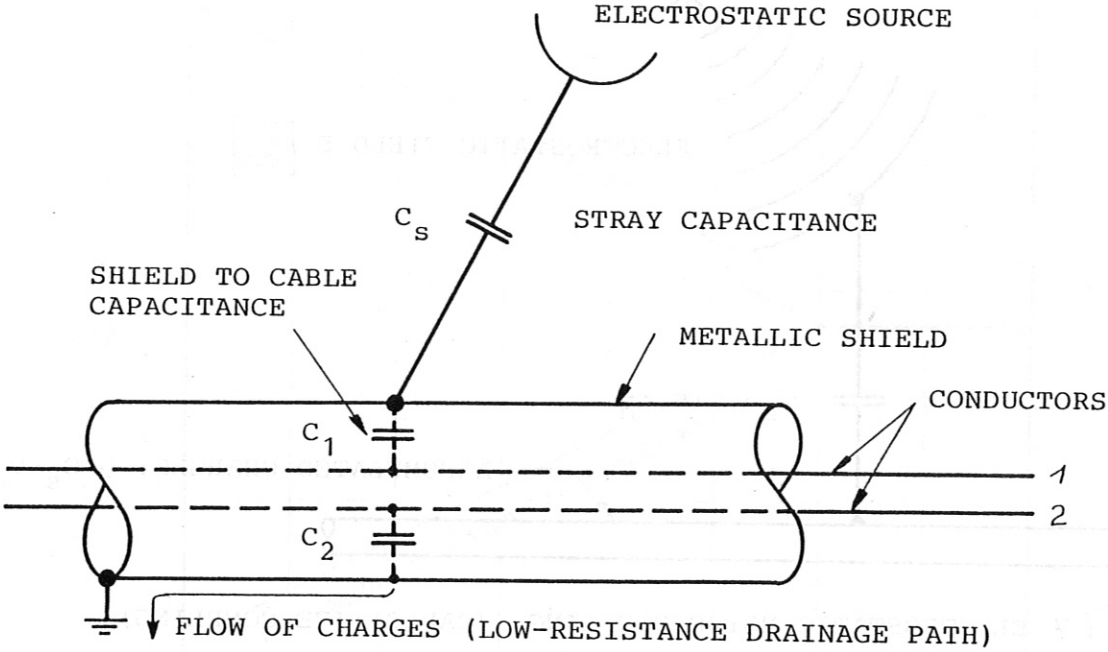

FIG.: 9 ELECTROSTATIC SHIELDING (FARADAY CAGE)

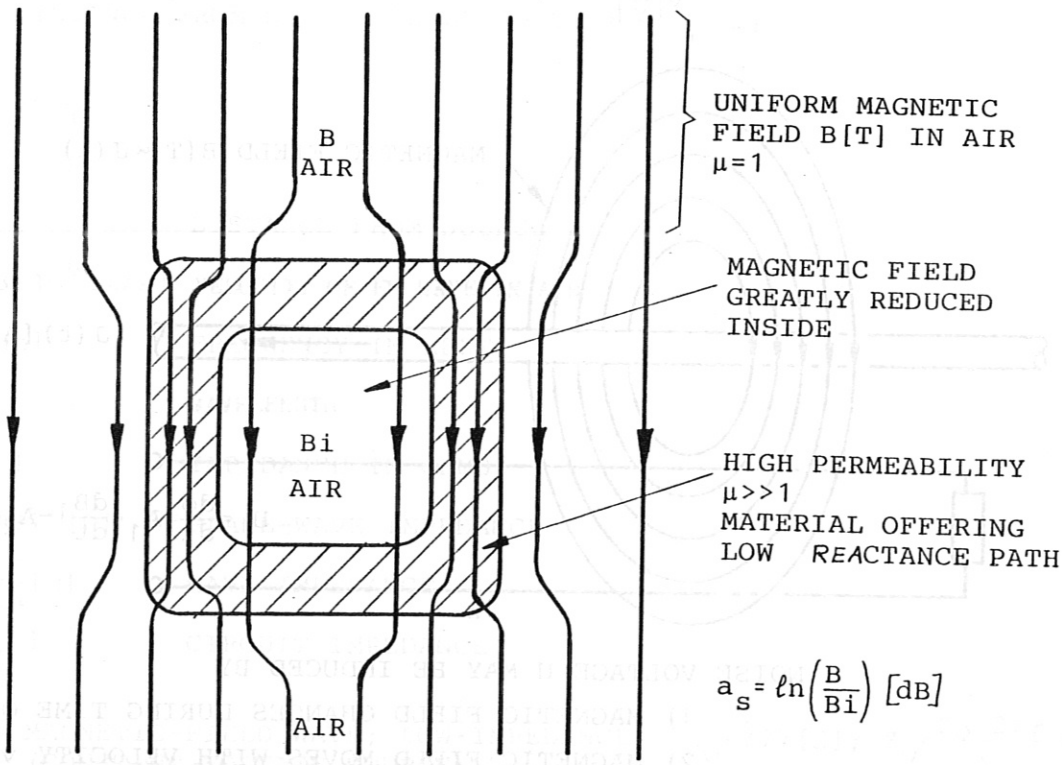

FIG.: 10 CROSS-SECTION OF A HOLLOW RECTANGULAR SOLID OF HIGH PERMEABILITY IMMERSED IN A UNIFORM MAGNETIC FIELD SHOWING DISTRIBUTION OF MAGNETIC FIELD LINES

COUPLING REJECTION

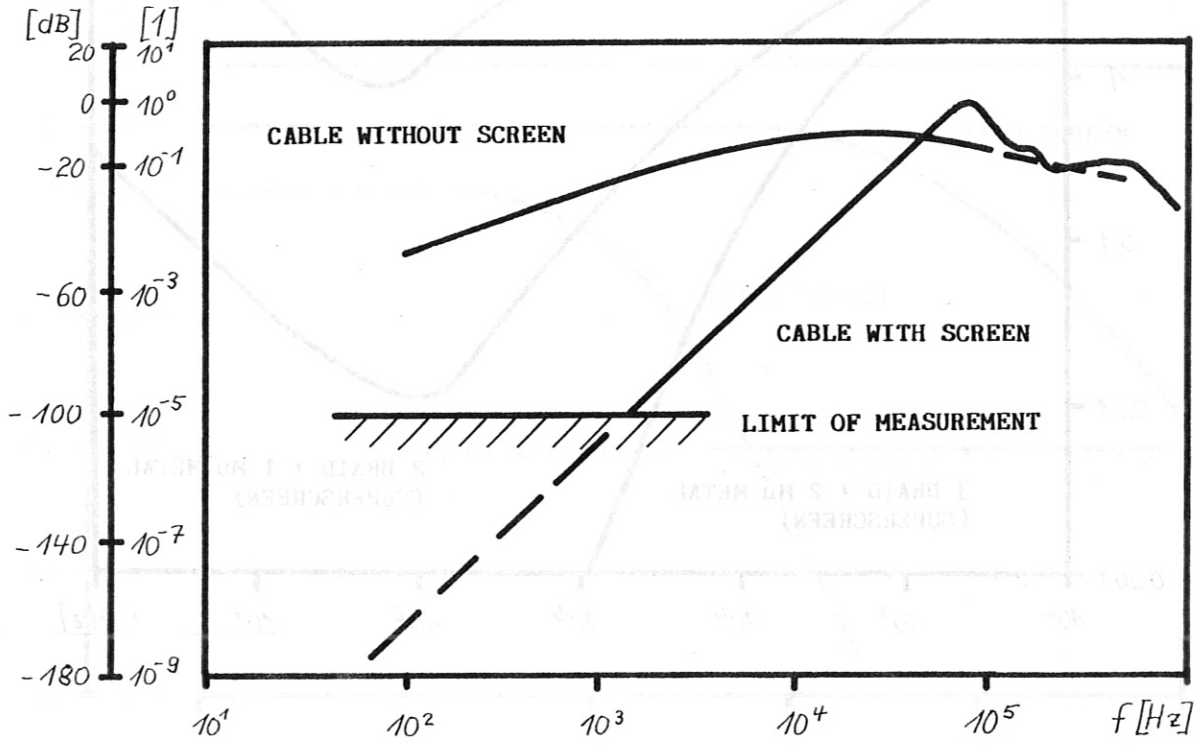

FIG. 11 COUPLING REJECTION AS A FUNCTION OF FREQUENCY f BY CAPACITIVE COUPLING

SURFACE TRANSFER IMPEDANCE $Z_T\left[\frac{m\Omega}{m}\right]$

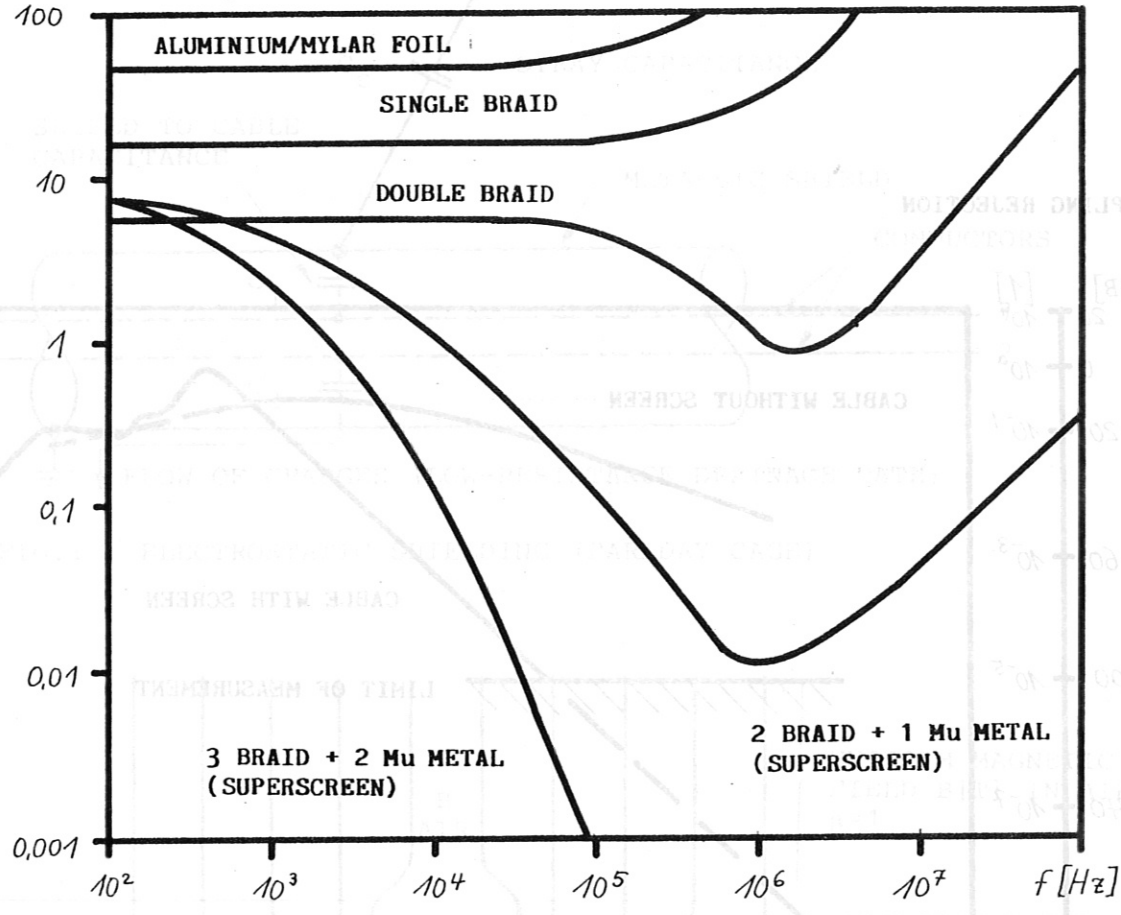

FIG. 12 VARIATION OF THE SURFACE TRANSFER IMPEDANCE WITH FREQUENCY f FOR DIFFERENT CABLE SCREEN CONSTRUCTIONS

COUPLING REJECTION

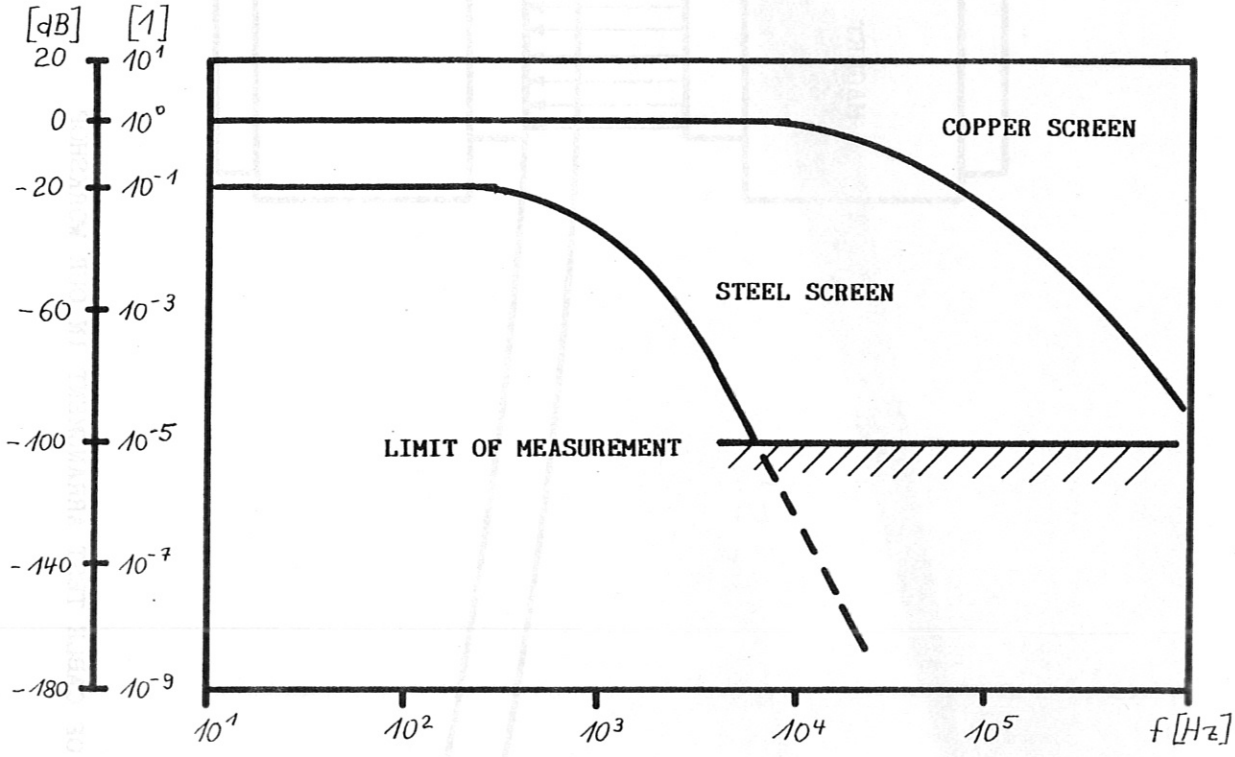

FIG. 13 COUPLING REJECTION AS A FUNCTION OF FREQUENCY f BY MAGNETIC COUPLING

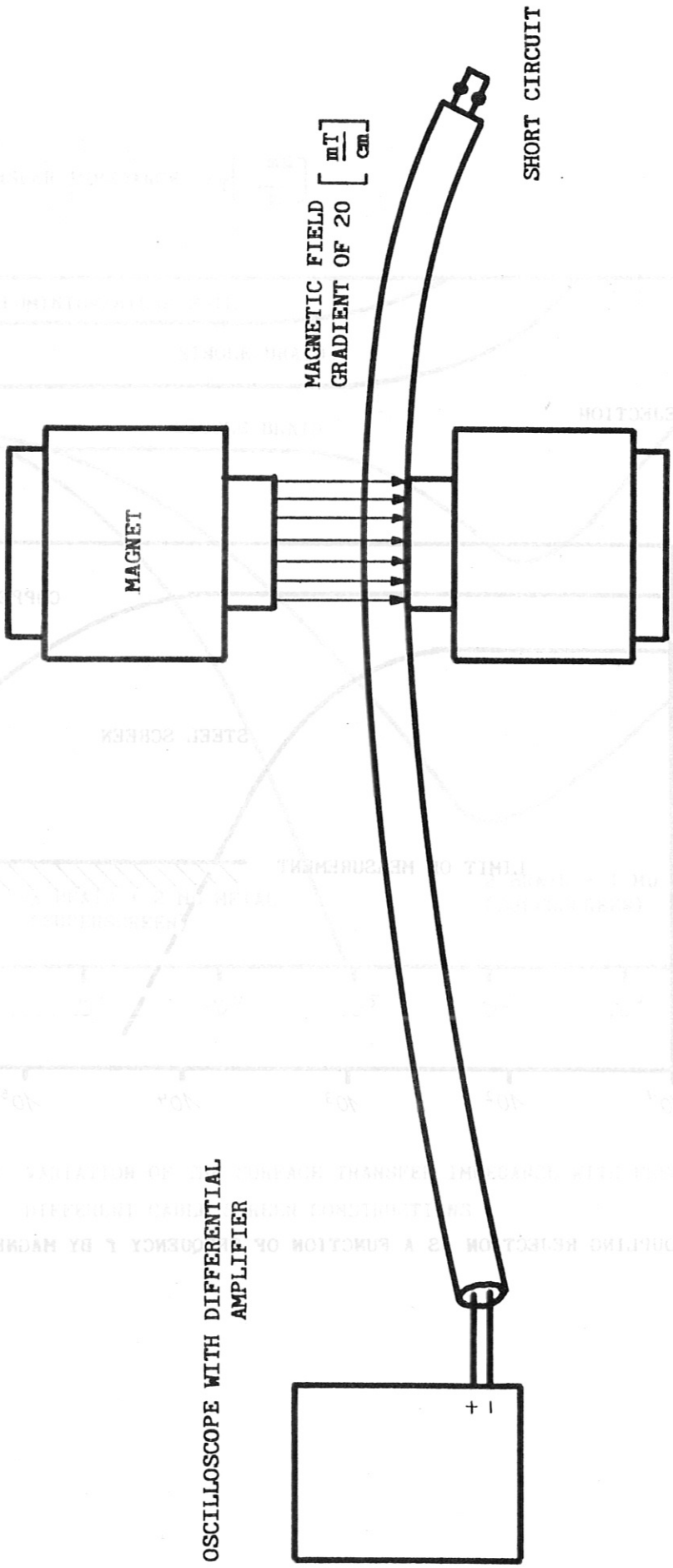

FIG. 14 SCHEMATICS OF CABLE TEST ARRANGMENT IN OUR WORKSHOP

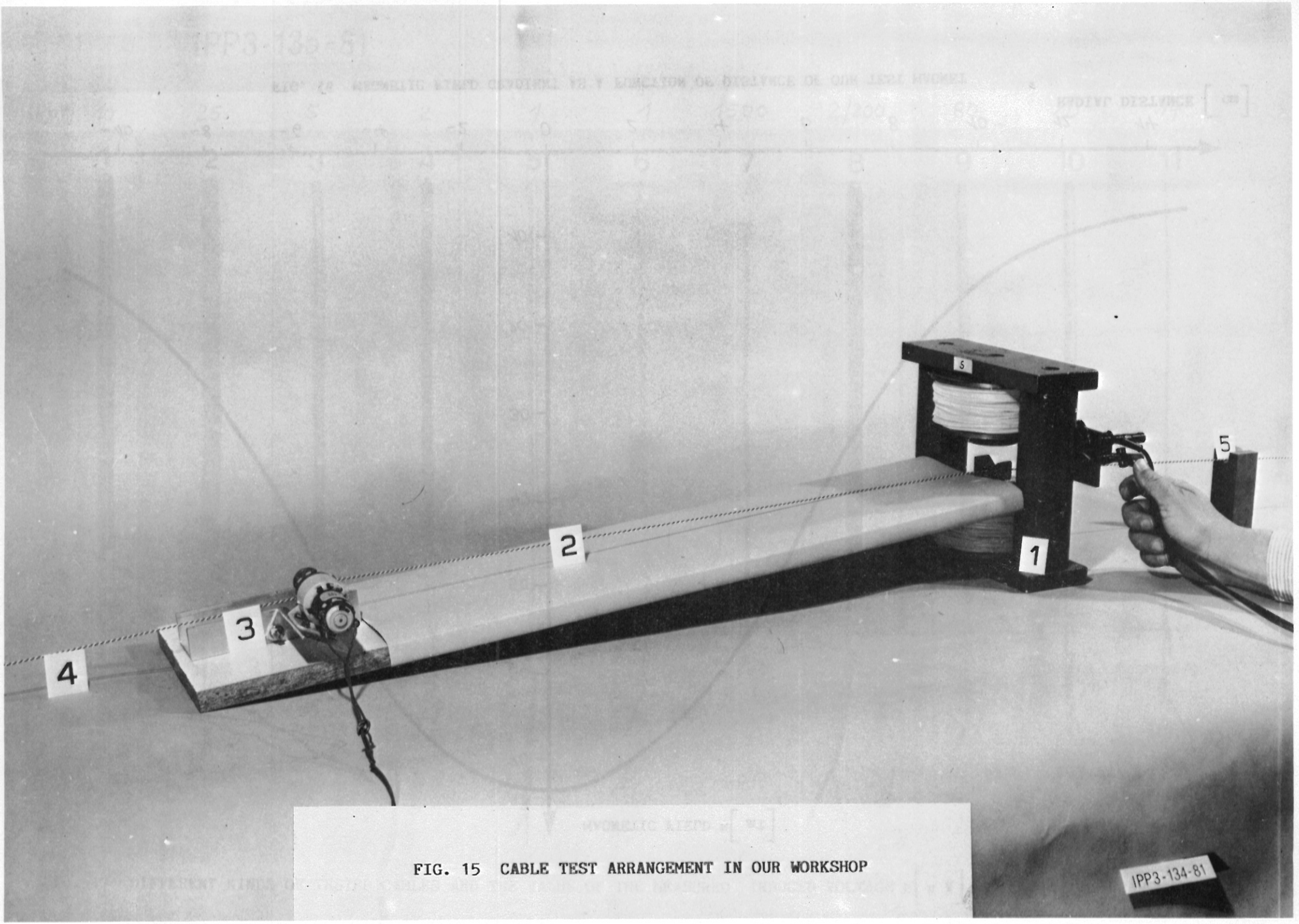

FIG. 15 CABLE TEST ARRANGEMENT IN OUR WORKSHOP

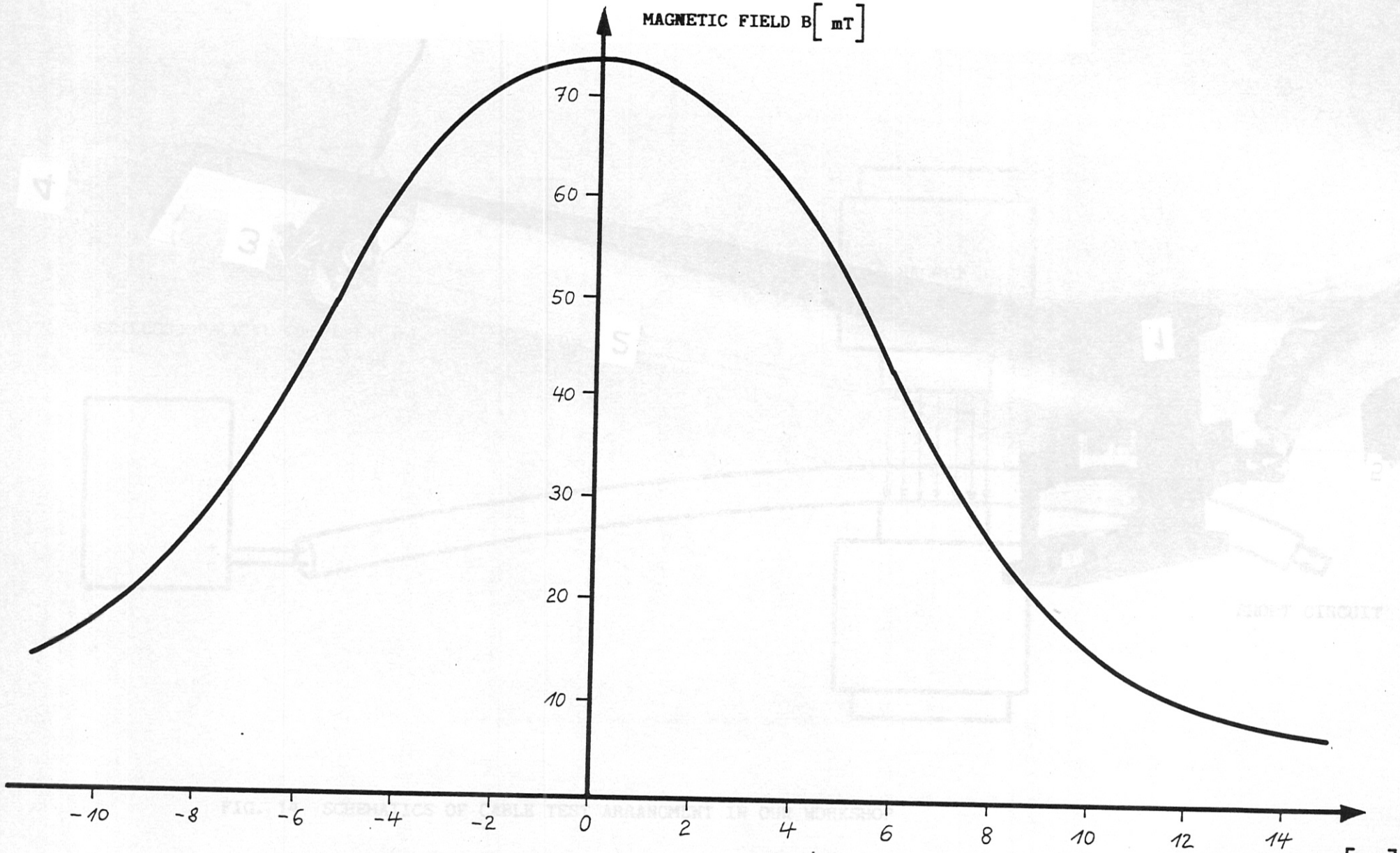

FIG. 16 MAGNETIC FIELD GRADIENT AS A FUNCTION OF DISTANCE OF OUR TEST MAGNET

IPP3-135-81

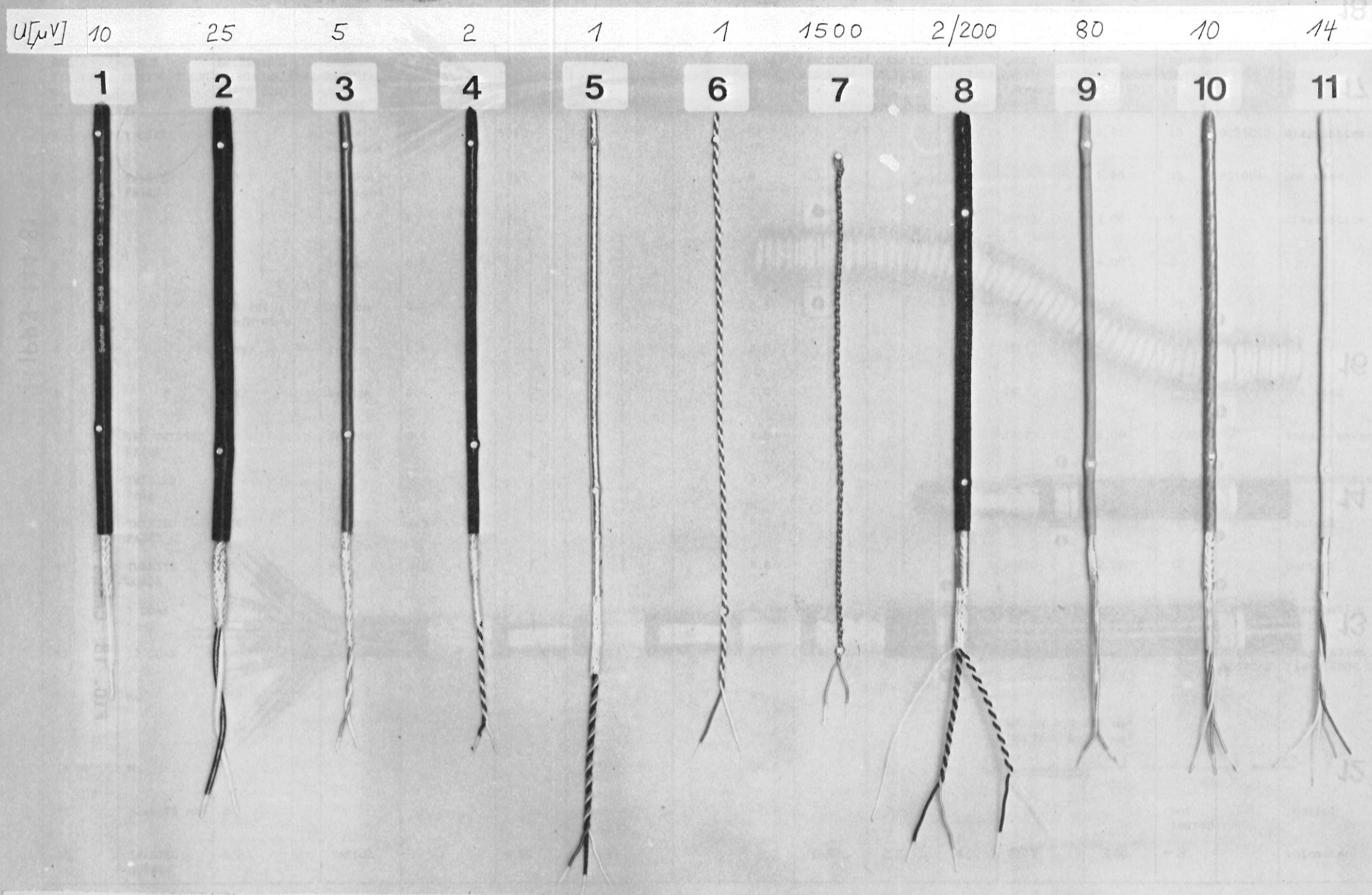

FIG. 17 DIFFERENT KINDS OF TESTED CABLES AND THE VALUE OF THE MEASURED INDUCED VOLTAGE U[μV] IN OUR TEST ARRANGEMENT

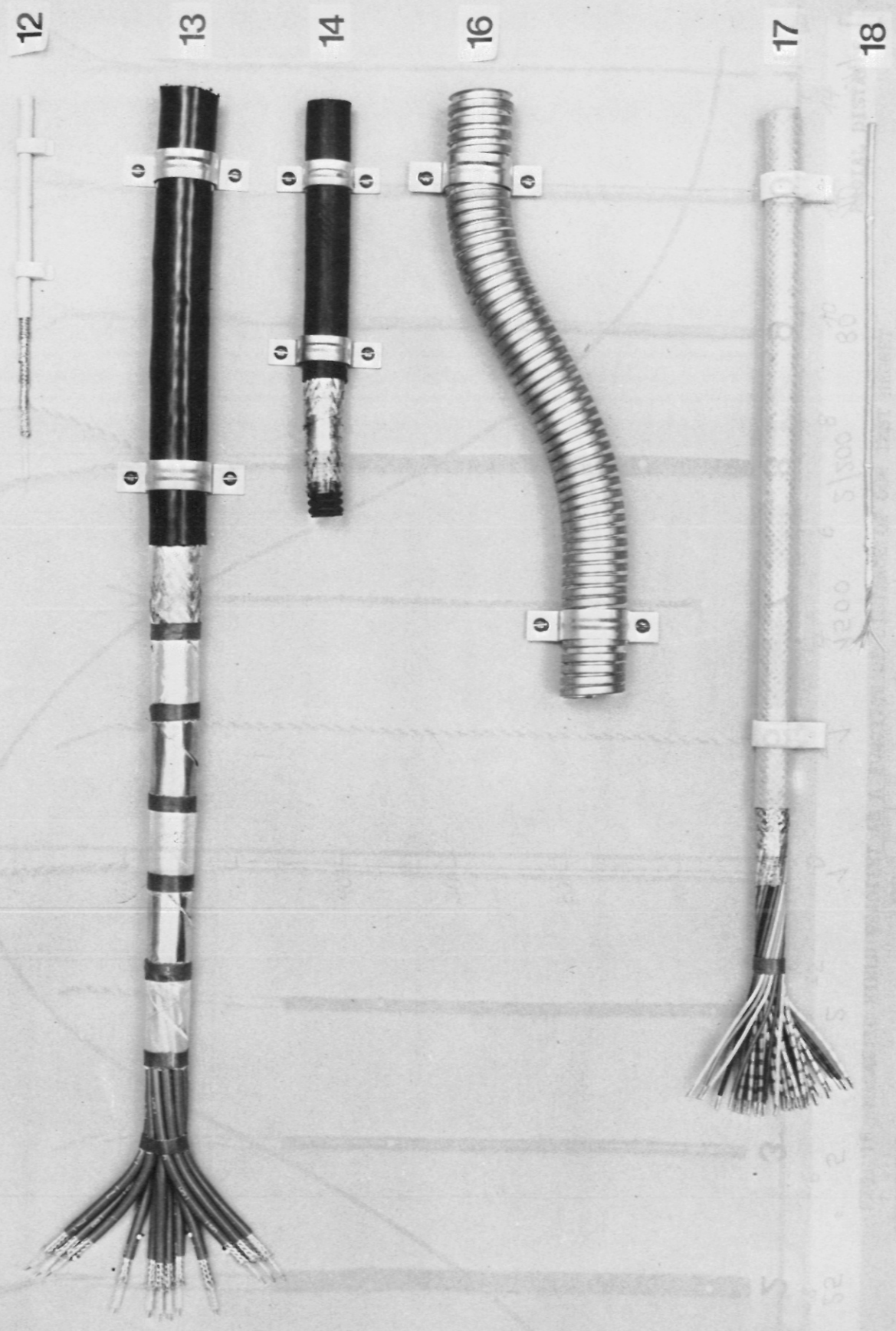

FIG. 18 CABLE AND MAGNETIC SHIELDING ARRANGEMENTS

SEE FIG.17/18 No.	CABLE CONSTRUCTION	SHIELDING: ALUMINIUM FOIL BRAID (Cu)	INSULATION MATERIAL	1 TWIST per cm CABLE LENGTH	CHARACT. IMPEDANCE [Ω]	CAPACITY [pF/m]	SHEATH Ø mm	FREQUENCY RANGE DC+...MHz	OPERATING VOLTAGE kV	TEST VOLTAGE kV	GAUGE AWG (Stranding)	COST per Meter DM (1981)	INDUCED VOLTAGE µV		USED FOR
1	1 COAX	B	Poly-ethylene	-	50±2	102	5	> 1	1	2,5		0,80	10	RG58C/U	diagnostics
2	TWISTED PAIRS	A/B	PVC/Poly-ethylene	5.3	78±7	80	6	0.5				1.80	25	RG108A	not used
3			Tefzel	1	-50	75/135	4				24(7)	3.00	5		diagnostics
4			Teflon	0.6			3.5				24(7)	4.00	2		
5		A/B and drain wire	Teflon	0.6			3.5				24(7)	4.00	-1		
6		NONE	Teflon	0.6			2.0				26(1)		-1		
7		NONE	Kapton	0.6			2.0				24(7)		1500		not used
8	TWO TWISTED PAIRS	A/B	Teflon	0.6			4.5				24(7)	8.00	2/200		strain gauge
9	TWISTED PAIRS	B		6			3.5				24(7)	4.00	80		thermocouple
10	TWISTED PAIRS	A/B	Tefzel	2.5			4.0				24(7)	3.00	10		control
11	TWISTED QUADS	B	PVC	2.5			4.0				24(7)	2.00	14		control
12	1 COAX	B			60 Ω	100	6.0	200	1	2.5			<1		diagnostics
13	12 COAX	A/B			50 Ω ± 2	102	27.0	200	1	2.5		40.00		MU/PO/ RG58C/U	diagnostics field <200 G
14	Mu	B					20.0				AWG 24 ≙ 0.227 mm² AWG 26 ≙ 0.141 mm²		-		
16	Mu	-					30.0						-		
17	32x0.75 mm²	B					17.0						not tested		control
18	TWISTED QUARDS	A/B	Teflon	1	- 50	75/135	3.2	0.5	0.3	1.0	26(7)	3,50	~3		bolometer

FIG. 19 LIST OF DIFFERENT CABLE TYPES

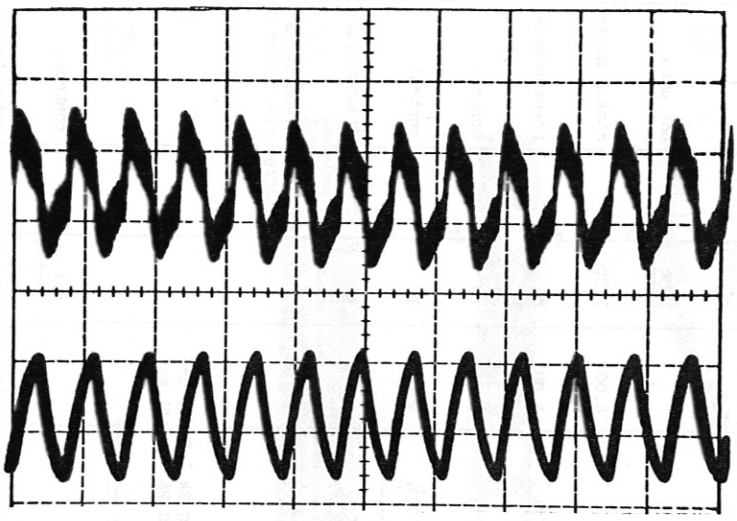

FIG. 20 OSCILLOGRAM OF A TESTED COAXIAL CABLE TYPE RG 58C/U

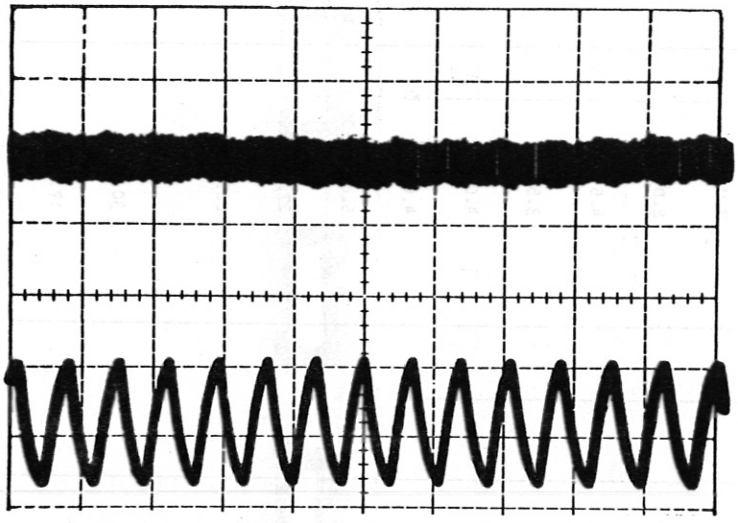

FIG. 21 OSCILLOGRAM OF A TESTED TEFLON CABLE WITH PAIRS OF TWISTED CONDUCTORS SIZE AWG 24 (ONE TWIST PER 5 mm OF CABLE LENGTH)

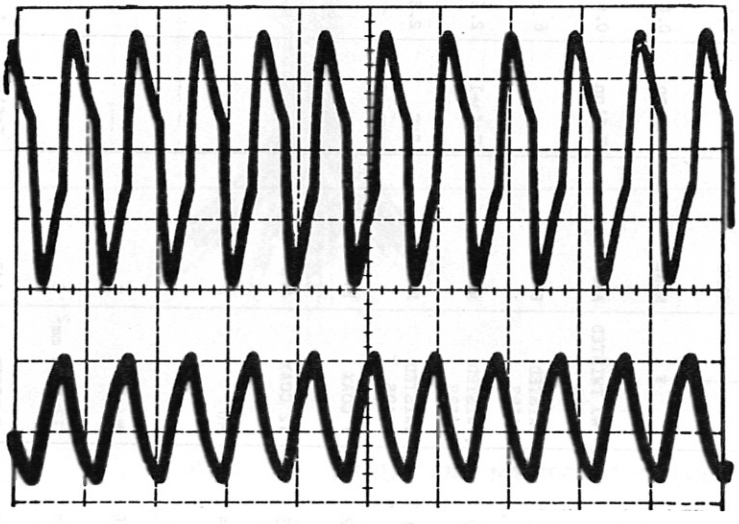

FIG. 22 OSCILLOGRAM OF A TESTED 4-CONDUCTOR CABLE WITH 2 TWISTED PAIRS

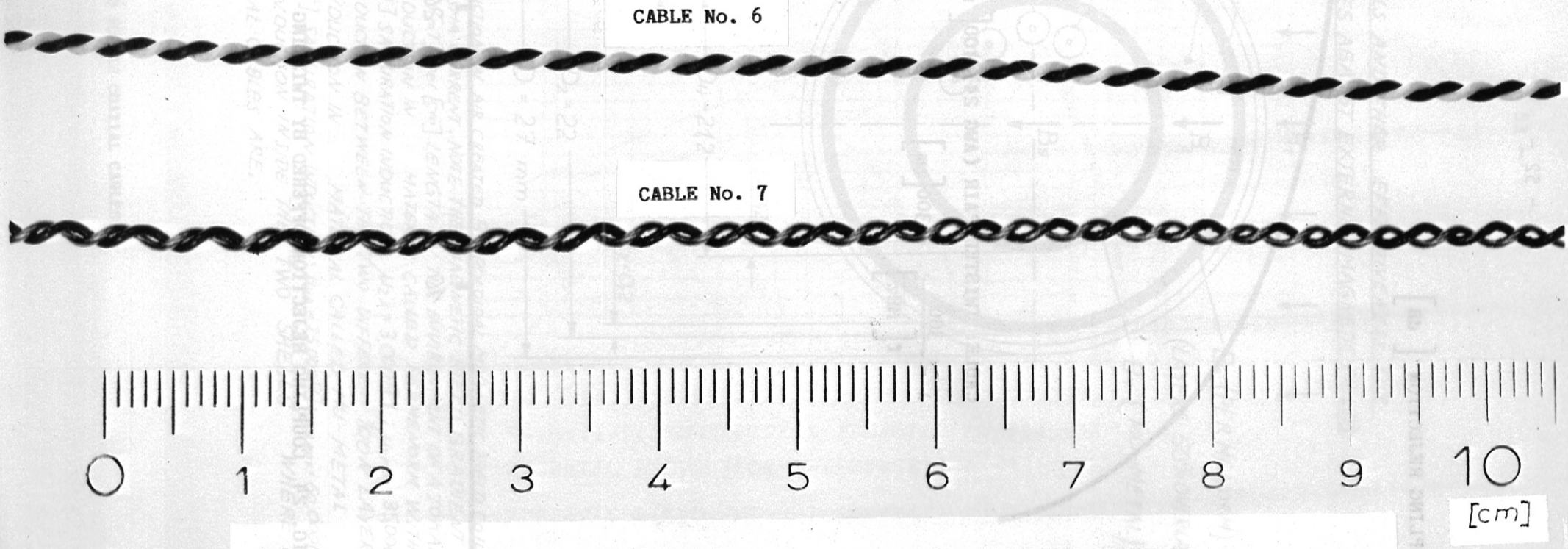

FIG. 23 THE UPPER PART OF THE PICTURE SHOWS A PAIR OF TWISTED CABLES WITH TEFLON INSULATION. THE LOWER PART SHOWS A PAIR OF TWISTED CABLES WITH KAPTON INSULATION

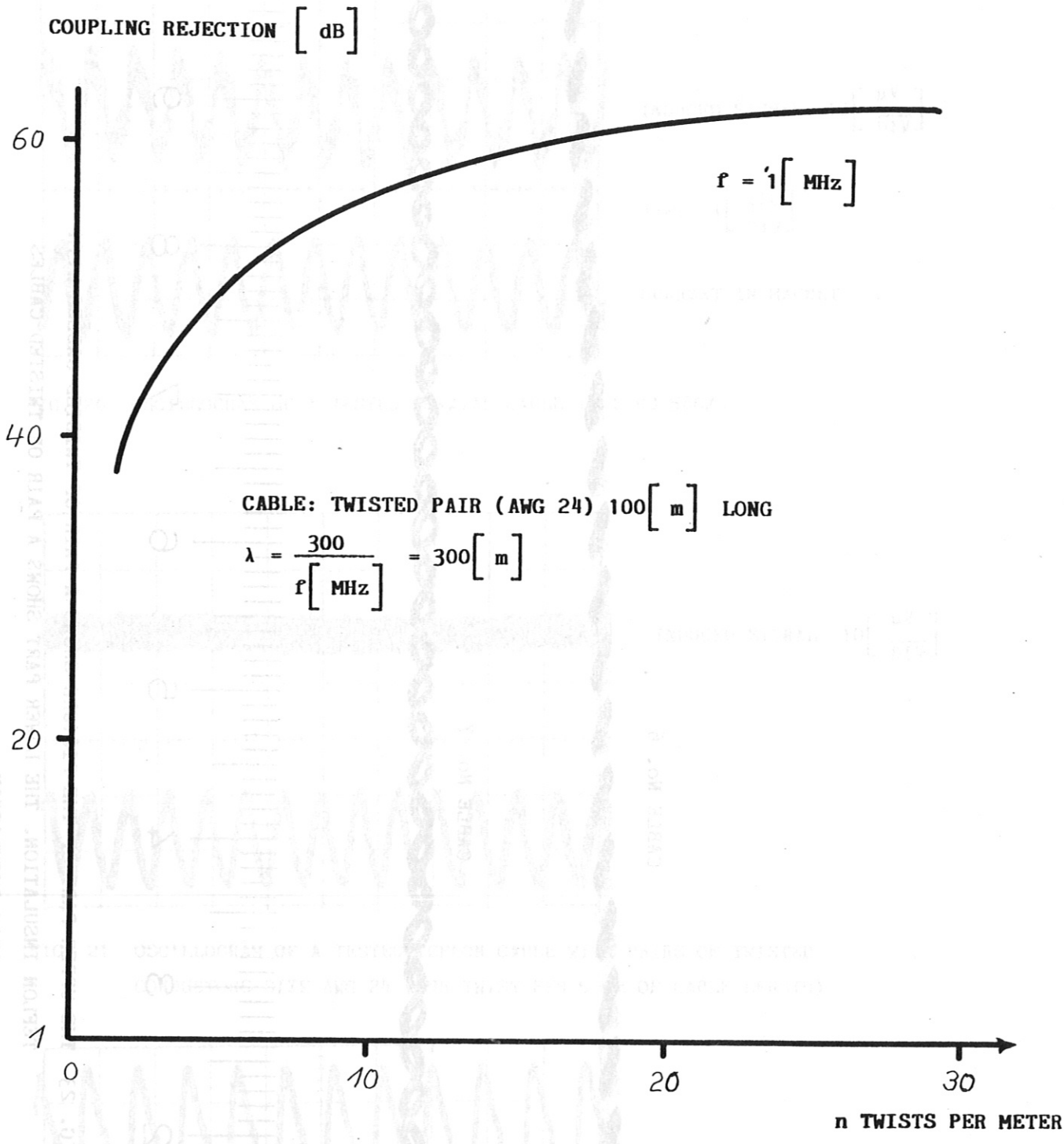

FIG. 24 COUPLING REJECTION OFFERED BY TWISTING WIRE PAIR

DOUBLE MAGNETIC SHELLS AND THEIR EFFECTIVENESS FOR SHIELD 12 COAXIAL CABLES AGAINST EXTERNAL MAGNETIC FIELDS

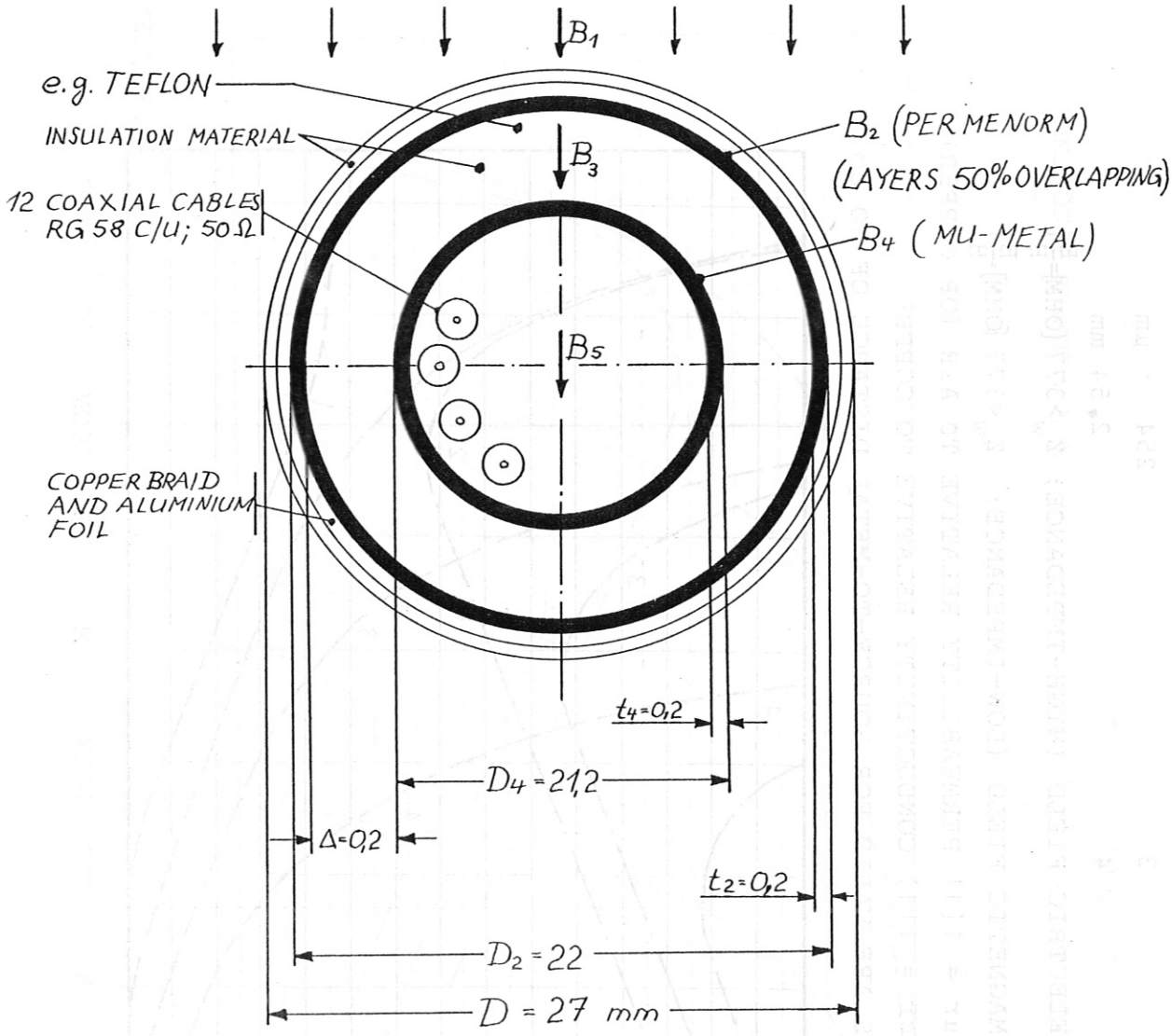

B_1 = 20 [mT] MAGNETIC INDUCTION IN AIR CREATED BY POLOIDAL MAGNETIC FIELD COILS AND THE PLASMA CURRENT. NOTE THE MAGNETIC FIELD GRADIENT OF ABOUT 20 [mT] per [cm] LENGTH IN THE ENVIRONMENT OF A TOKAMAK.

B_2 MAGNETIC INDUCTION IN MATERIAL CALLED PERMENORM WITH B_{2S} = 1,35 [T] SATURATION INDUCTION; μ_{2A} = 3,000 [1]; μ_{2max} = 35,000 [1].

B_3 MAGNETIC INDUCTION BETWEEN THE TWO DIFFERENT IRON LAYERS.

B_4 MAGNETIC INDUCTION IN MATERIAL CALLED MU-METAL B_{4S} = 0,8 [T] SATURATION INDUCTION; μ_{4A} = 25,000 [1]; μ_{4max} = 60,000 [1].

B_5 MAGNETIC INDUCTION INSIDE THE TWO SHELLS WHERE THE 12 COAXIAL CABLES ARE.

FIG. 25 MAGNETIC SHIELD FOR 12 COAXIAL CABLES

PARAMETER OF CURVE 1 THICKNESS OF METAL IS 2.43 µm

" 2 " 25.4 µm

3 254 µm

4 2.54 mm

—·—·— ELECTRIC FIELD (HIGH-IMPEDANCE; $Z_w > 377$ [OHM] $= \frac{E}{H}$)

— — — — MAGNETIC FIELD (LOW-IMPEDANCE; $Z_w < 377$ [OHM] $= \frac{E}{H}$)

µr = 1[1] PERMEABILITY RELATIVE TO AIR (OR COPPER)

σr = 1[1] CONDUCTIVITY RELATIVE TO COPPER

ALL FIGURES ARE VALID FOR SOURCE-TO-METAL DISTANCE OF 10 cm

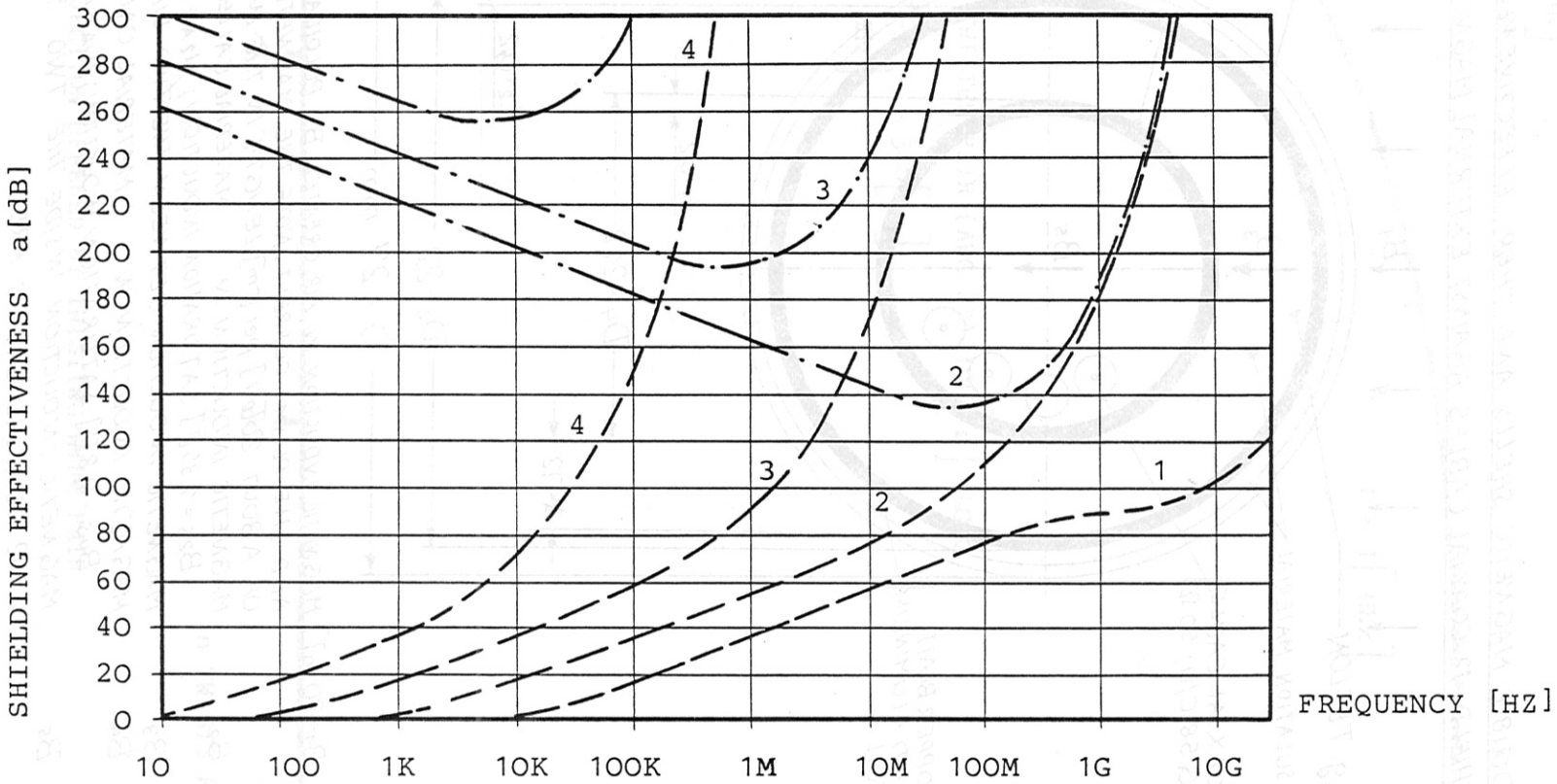

FIG.:26.0 SHIELDING EFFECTIVENESS OF COPPER VERSUS FREQUENCY

$\mu_r = 1$; $\sigma_r = 1$

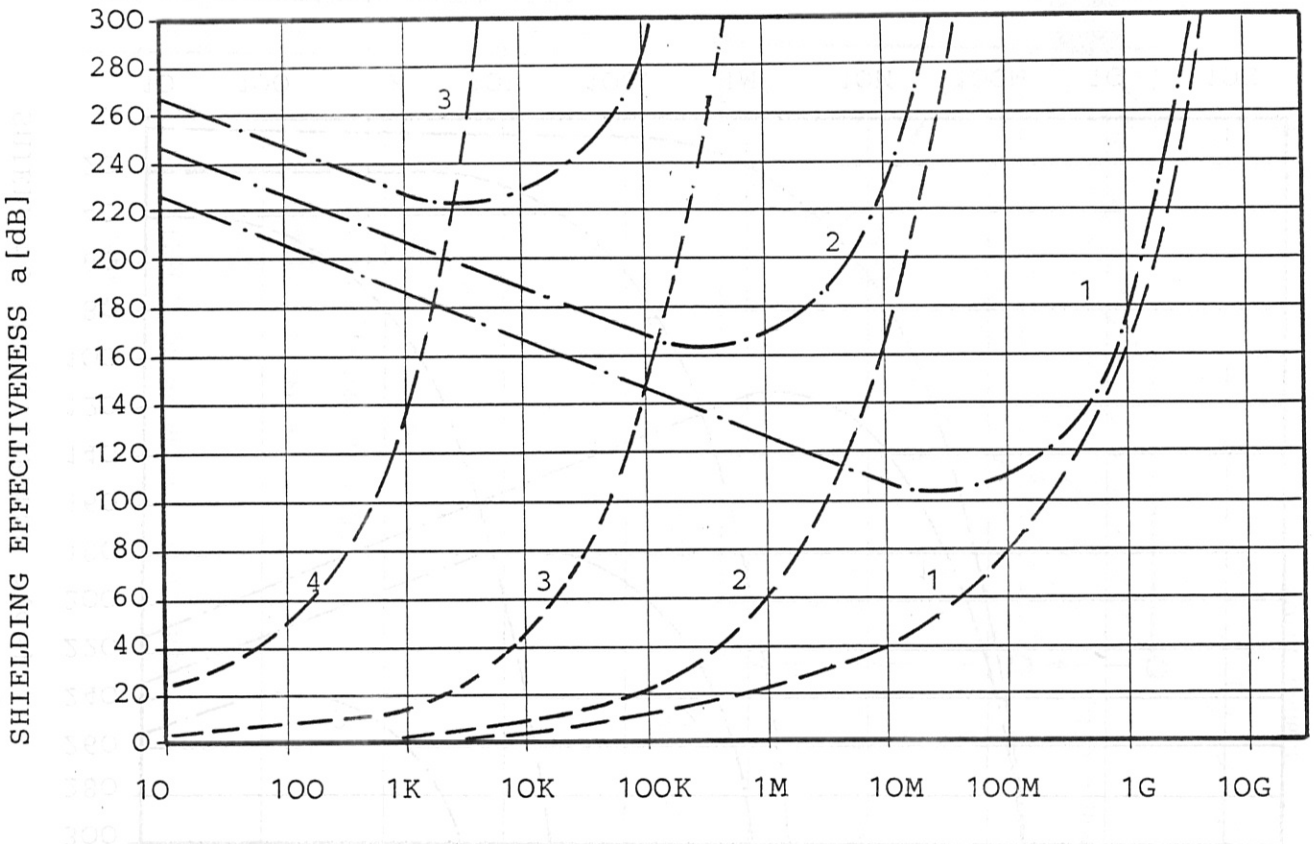

FIG.: 26.1 SHIELDING EFFECTIVENESS OF IRON VERSUS FREQUENCY

$\mu_r = 1000$; $\sigma_r = 0.17$

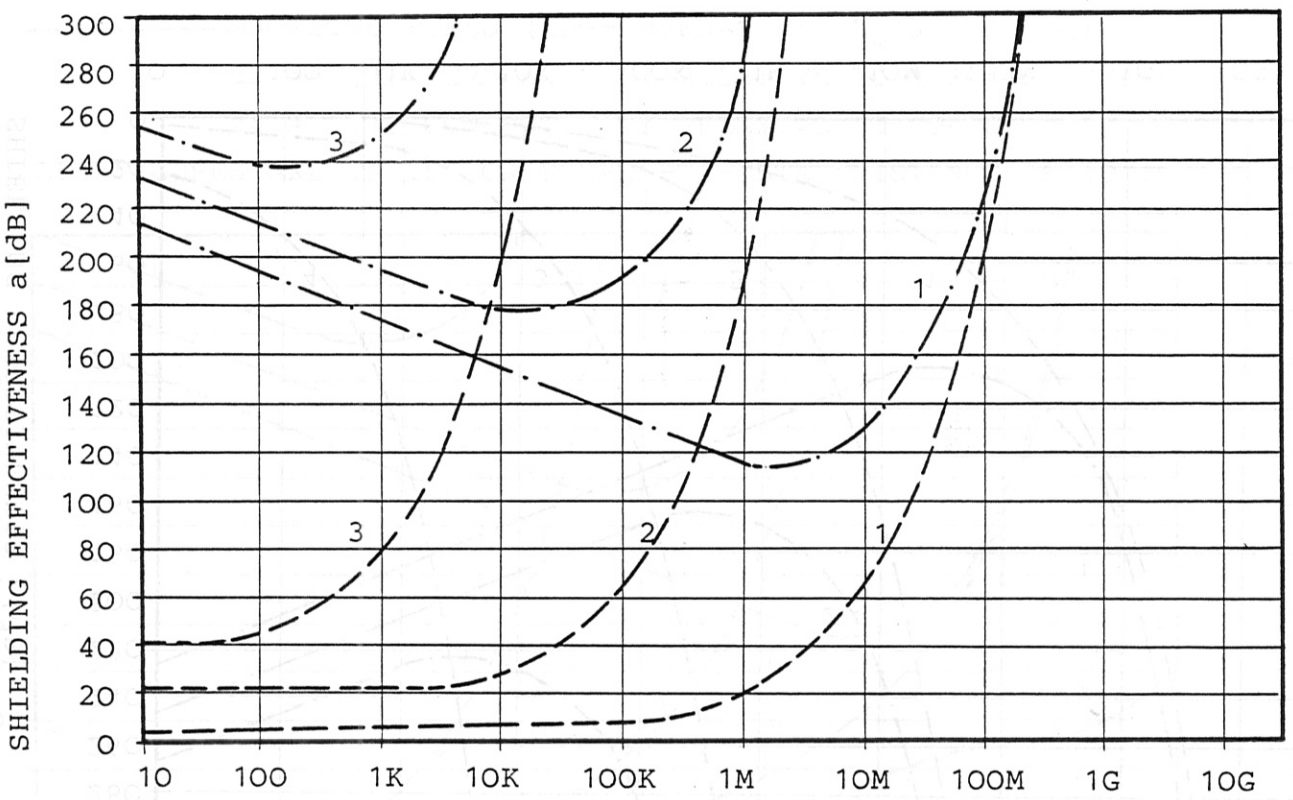

FIG. 26.2 SHIELDING EFFECTIVENESS OF MATERIAL WITH HIGH PERMEABILITY VERSUS FREQUENCY

$\mu_r = 80{,}000$; $\sigma_r = 0.04$

$$U'_{1,2} = \sum Aa \frac{d(B_{1,2})}{dt} - \sum Ab \frac{d(B_{1,2})}{dt} = U_{DMV} \; ; \; U'_{1,2} \ll U_{1,2}$$

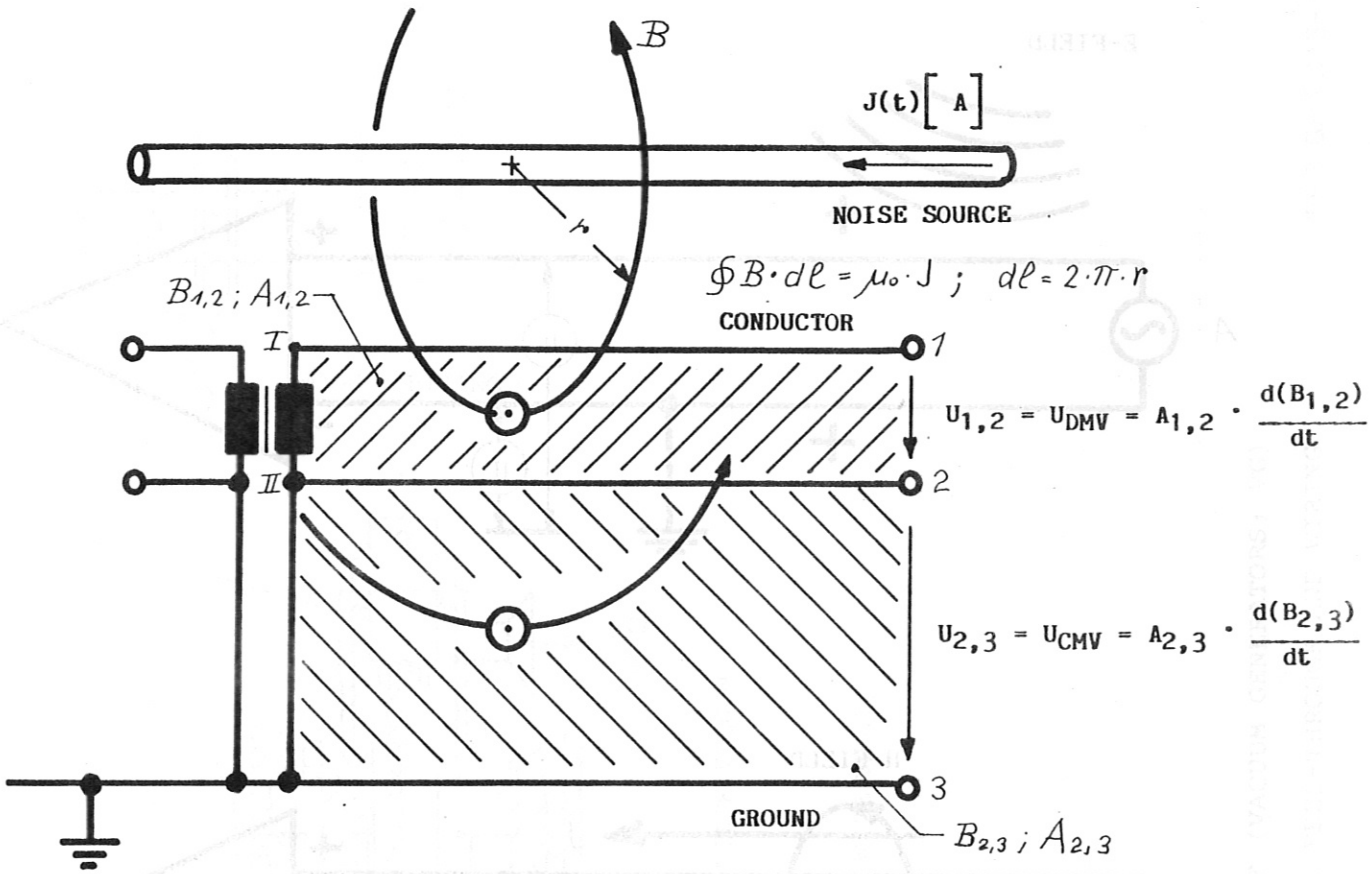

Ua,Ub	[V]	INDUCED VOLTAGE
Us	[V]	SIGNAL
J	[A]	CURRENT
B	[T]	MAGNETIC FIELD
A	[m^2]	AREA OF MAGNETIC FLUX
n	[1]	TWIST OF CABLE
t; dt	[S]	TIME
dl	[m]	LENGTH OF MAGNETIC FIELD LINES
r	[m]	RADIUS

SEE UPPER PICTURE

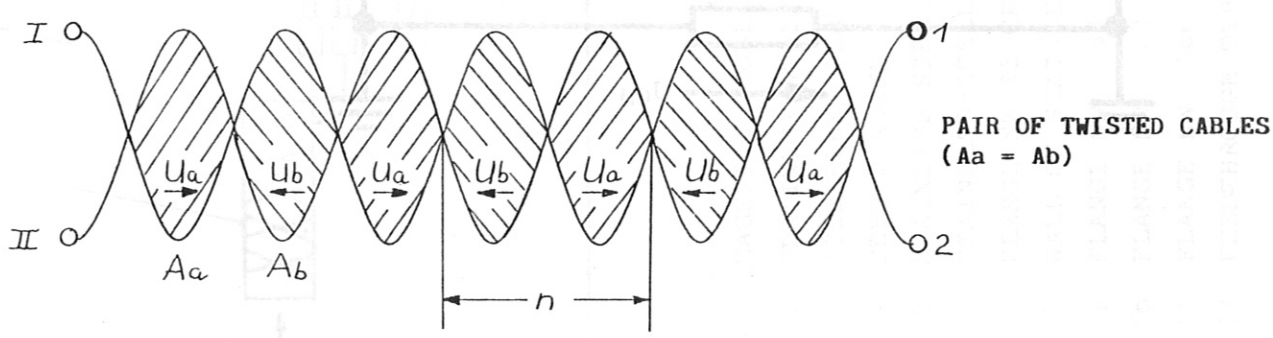

FIG. 27 DEVELOPMENT OF COMMON-MODE VOLTAGE U_{CMV} AND DIFFERENTIAL-MODE VOLTAGE (U_{DMV})

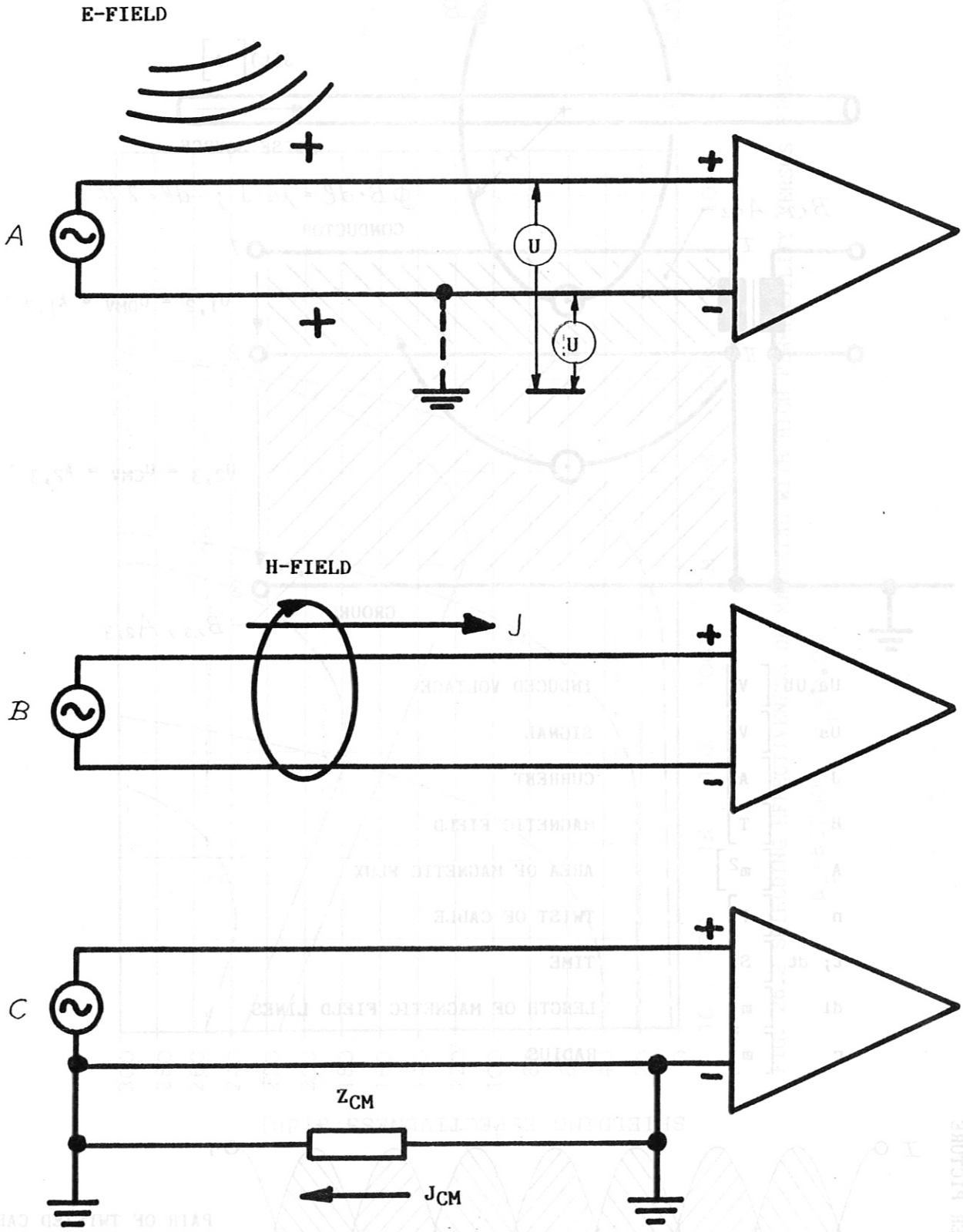

FIG. 28 THREE SOURCES OF COMMON-MODE NOISE

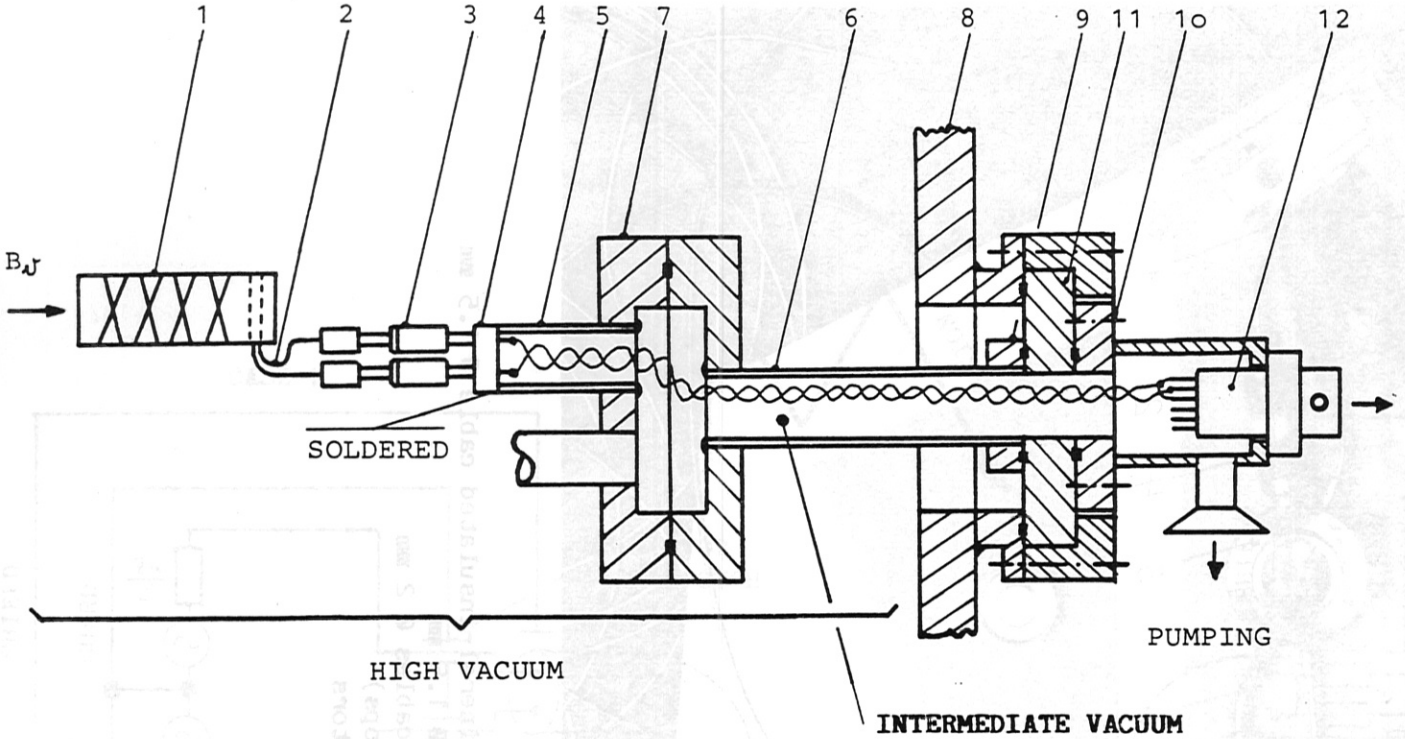

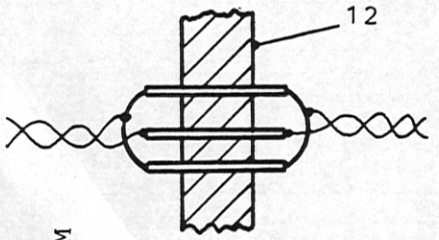

TO CONTROL ROOM

TO REDUCE PICK-UP SIGNALS USE 3-PIN ARRANGEMENT

1 MAGNETIC PROBE
2 PLATINUM-RHODIUM WIRE
3 SOLDERLESS TERMINAL TYPE CC (COMPONENTA OTTOBRUNN, W. GERMANY)
4 FEED-THROUGH
5 STAINLESS-STEEL TUBE DIAMETER 6/4 mm
6 STAINLESS-STEEL TUBE DIAMETER 15/13 mm
7 FLANGE NW 35 CF
8 WALL OF STAINLESS-STEEL VACUUM VESSEL
9 FLANGE NW 63 CF
10 FLANGE NW 63 CF
11 FLANGE NW 100 CF
12 FEEDTHROUGH TYPE EFT55; 7A; 700 V; 55 PIN; NW 35 CF (VACUUM GENERATORS; VG)

FIG. 29 MAGNETIC PROBE WITH FEED-THROUGH AND WIRING

IPP3 GHT 313-80

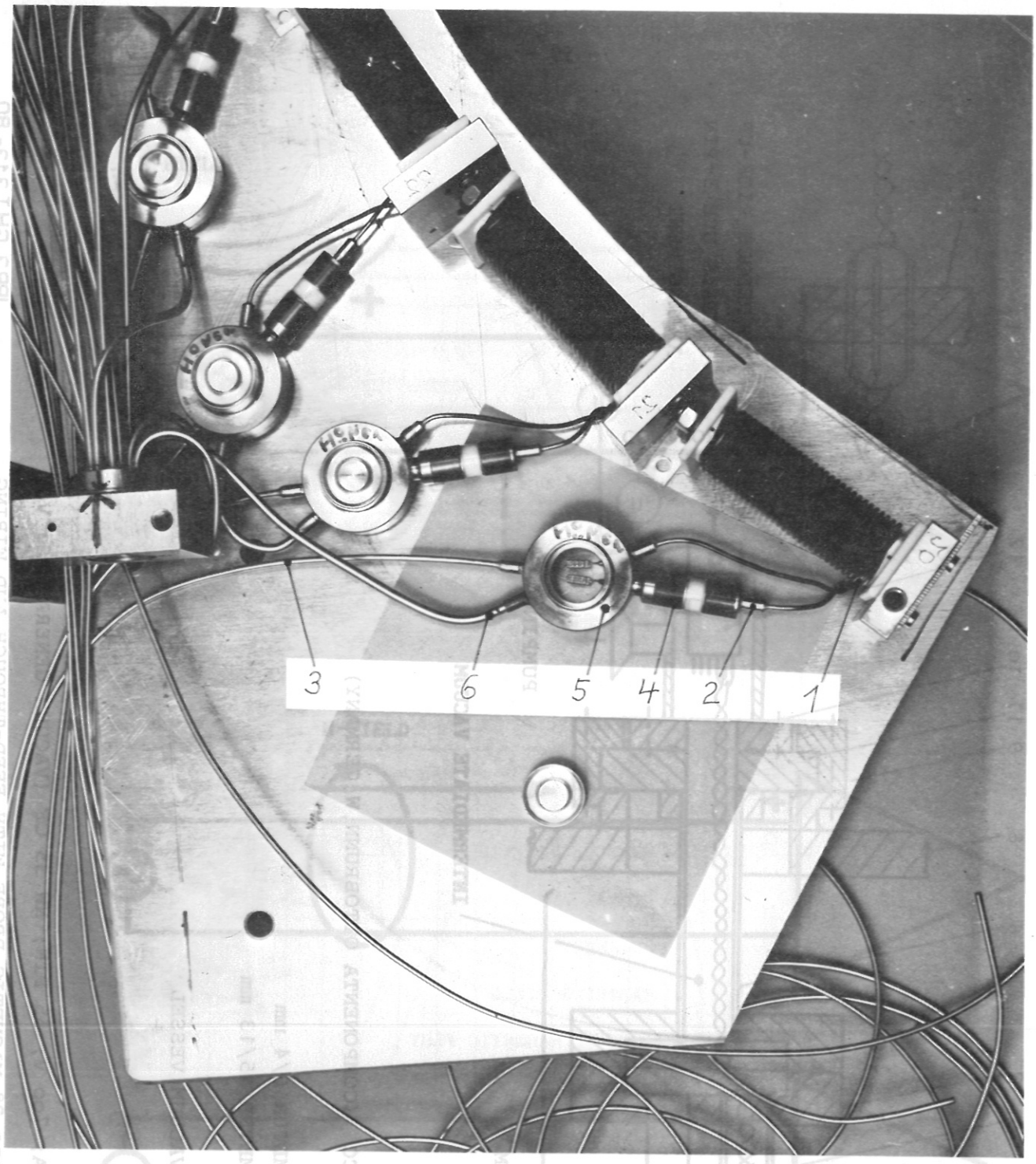

1. Magnetic probe made of coaxial mineral-insulated cable Ø 1.5 mm
2. Coaxial mineral-insulated cable Ø 1.5 mm
3. Two-conductor mineral-insulated cables Ø 2 mm
4. Feed-through (to avoid closed loops)
5. Terminal box with crimped conductors
6. Pumping tube Ø 4 mm

FIG. 30 MAGNETIC PROBE CONNECTED WITH MINERAL-INSULATED CABLES (MgO)

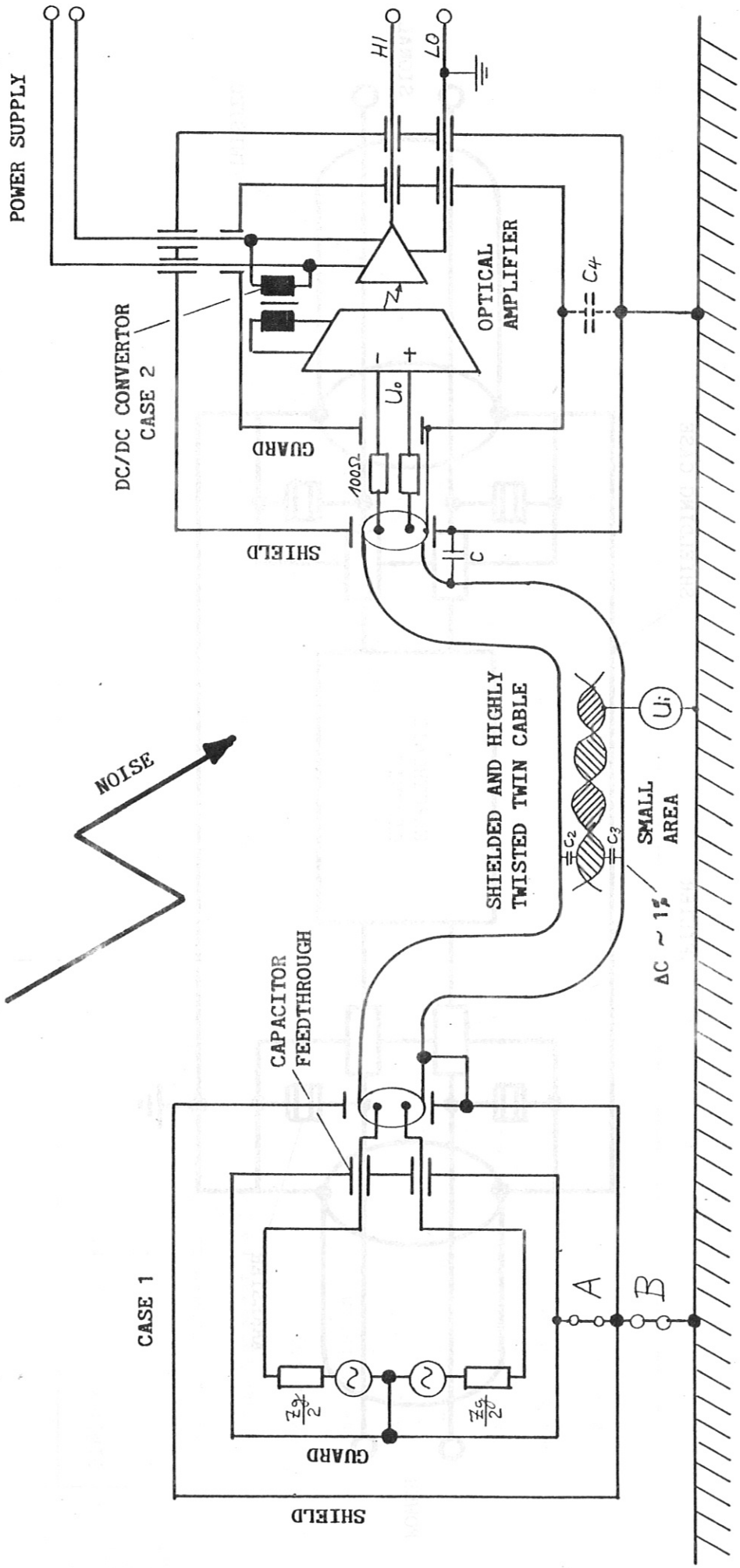

FIG. 31 EXAMPLE OF AN ELECTRIC CIRCUIT IN AN EXPERIMENTAL ENVIRONMENT

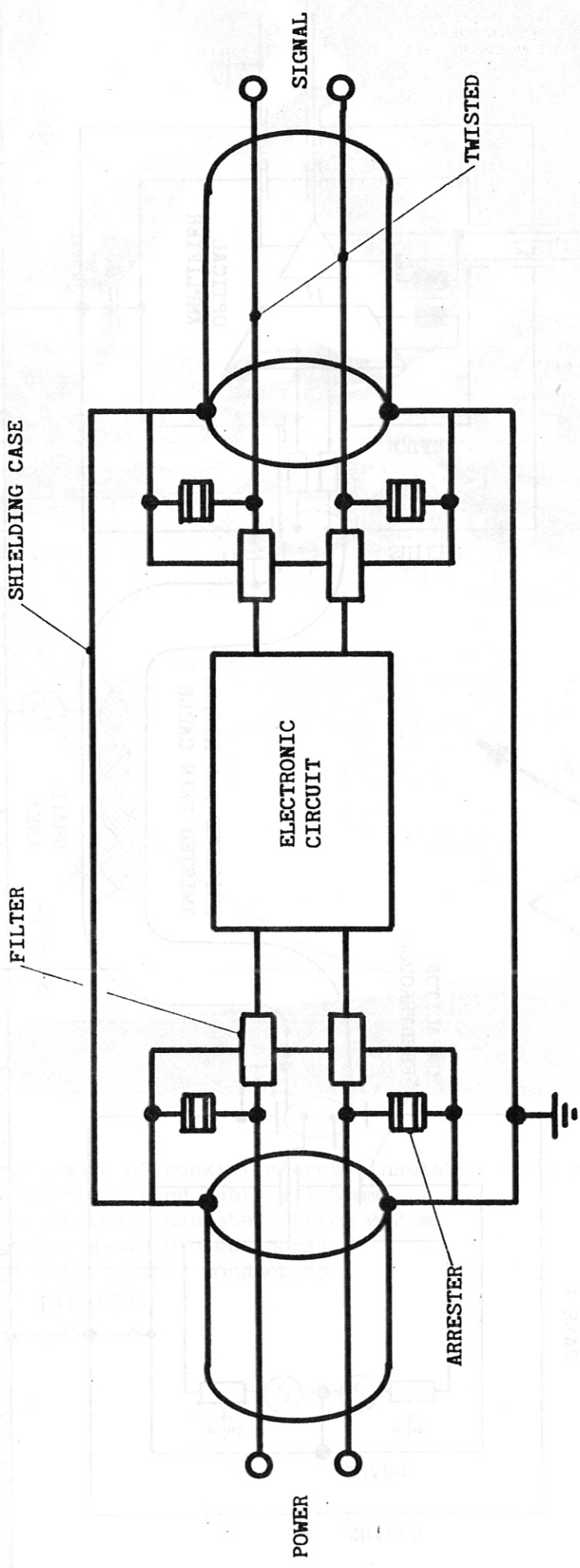

FIG. 32 ELECTRONIC CIRCUIT PROTECTED BY SURGE ARRESTORS AGAINST SPURIOUS VOLTAGE SIGNALS

	P.E. Polyethylene	PVC Polyvinyl	ETFE Tefzel	PTFE	FEP	Polyimide Kapton	Victrex PEEK*	Tedur
Dielectric constant at 10^3 Hz	2.3	3.5	2.6	2	2	3.5	3.3	4
Loss factor at 10^3	0.0005	0.08	0.0008	0.0002	0.0003	0.003	0.0003	0.0007
Breaking voltage in [kV/0.1 mm]	4	3	3	2	2.5	5	1.9	
Maximum temperature [°C]	+75	+85	+150	+260	+200	+200	+240	+240
Flexibility	weak	good	fair	good	good	medium	weak	weak
Flame resistance	burns	self-exciting	self-exciting	non	non	non	non	
E-Module [N/mm^2]			13700	6600	6600	3 GPa	8500	19000
Thermal expansion [$10^{-6}/°K$]					20	47	20	
Limited oxygen index [%] LOI	20	30	30	95	95	48	44	48
Density [g/cm^3]	0.92	1.3	1.7	2.16	2.16	1.9	1.4	1.8
X-rays (γ) [rad]	10^8	10^7	10^8	10^5	10^7	10^8	10^9	

* Polyetheretherketon

FIG. 33 INSULATION MATERIAL FOR CABLES

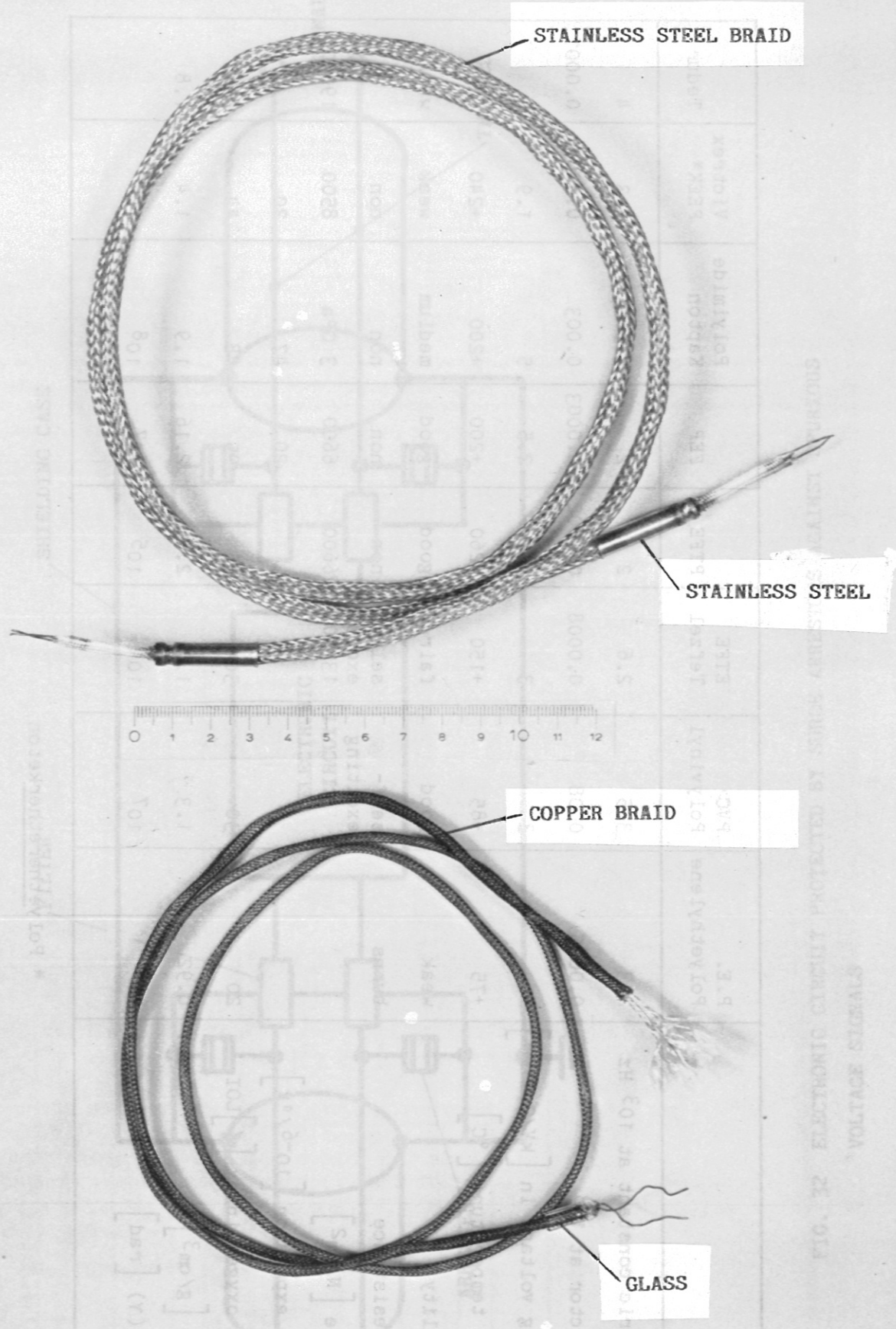

FIG. 34 PAIR OF TWISTED CABLES WITH GLASS SILK INSULATION

FIG. 35 SPECIFICATION FOR SILK-INSULATED CABLES

Spezifikation Sondenkabel / Probe Cable Specification

Typ/Type	JK2L-E	K12L-T	SK2L-T	SK2L-E	SK1L-E	SK1L-EU
Isolation/ Insulation	1)Glasseide glass silk	Glasseide glass silk	Micafolie Glasseide mica foil glass silk	Micafolie Glasseide mica foil glass silk	Micafolie Glasseide mica foil glass silk	Micafolie Gasseide mica foil glass silk
Leiter Werkst./ Conductor material	E-Kupfer E-copper	NiCr-Ni Thermoelementwerkstoff Thermocouple/DIN 43710	NiCr-Ni	NiCr	Ni-Cr	Ni-Cr
Verdrillungen/ Twist	50PH	50PH	25PH	25PH	--	--
Drahtdurchm./ Diameter	0.5 mm	0.3 mm	0.5 mm	0.5 mm	0.5 mm	0.5 mm
M a n t e l / S h e a t i n g						
Werkstoff Material	E-Kupfer E-copper		Rostfreier Stahl, W.Nr. 1.4301 od. W.Nr. 1.4435 Stainless Steel, W.No. 1.4301 or W.No. 1.4435			
Durchm./Diam.	0.2 mm	0.2 mm	0.2 mm	0.2 mm	0.2 mm	0.2 mm
Bedeckungsgrad/ Covering grade	ca. 75 %	ca. 75 %	ca. 75 %	ca. 75 %	ca. 75 %	ca. 75 %
A b m e s s u n g e n / D i m e n s i o n s						
Kabeldurchm./ Cable diam.	3.5 mm	3.5 mm	6.0 mm	6.0 mm	4.0 mm	4.0 mm
Kabellänge/ Cable length	max. 250 m	max. 250 m	max. 250 m	max. 250 m	max. 250 m	max. 250 m
Mantelab-schluß/ Sheathing end	Glasperle, beidseitig aufgeschmolzen: Hülse aus rostfreiem Stahl, beidseitig aufgeschweißt/Glass bead, melted onto both ends; stainless-steel sleeve, welded onto both ends					
Länge der Anschlußdrähte/ Length of wires	ca. 30 mm	ca. 30 mm	ca. 30 mm	ca. 30 mm	ca. 30 mm	ca. 30 mm
Verwendung/ Application	Signalleitung/ Indicator conductor	Thermoelementleitung Grundwerte der Thermospannung/ thermocouple conductor basic figure of the thermovoltage according DIN 43710			Signalleitung/ indicator conductor	
E i n s a t z g e b i e t / f i e l d o f a p p l i c a t i o n						
Vakuum/Vacuum	800 k	800 K	900 K	900 K	900 K	900 K
Luft/Air	450 K	450 K	950 K	950 K	950 K	950 K
Biegeradius/ Bend radius	10 mm	8 mm	25 mm	25 mm	25 mm	25 mm
Spannungs-festigkeit/ Dielectric strength	1 kV DC	1 kV DC	2 kV DC	2 kV CD	2 kV CD	2 kV DC
Permeabilität/ Permeability	1.0	≤1.05	≤1.05	≤1.05	≤1.05	≤1.05
Wellenwider-stand/Wave resistance	75 Ohm	---	---	75 Ohm	75 Ohm	75 Ohm

1) Auf Wunsch mit Micafolie/on request with Mica foil

For more information please contact:
Weitere Information durch:
Sulzer Brothers Ltd.
Boiler and Nuclear Engineering Division
Ch-8401 Winterthur
Switzerland
Phone 052-81 34 22
Telex 896 060 033
Fax 052-22 04 76

Allgemeine Hinweise/General remarks

Aufbau/ Structure	Leiterdrähte einzeln mit Micafolie (auf Wunsch) einfach umsponnen, mit Glasseide doppelt umsponnen, miteinander verdrillt, gemeinsam mit Glasseide einfach umflochten und mit Drahtgeflecht umhüllt. Querschnitt oval./ Conductors, each singly braided with mica foil (on request) and doubly braided with glass silk, twisted together, and singly braided with glass silk, and sheathed in wire gauze.
Behandlung/ Treatment	Ausgegast im Vakuum bei 0.1 Pa und 600 K während 6 Std./ Vacuum outgassing at 0.1 Pa and 600 K for 6 hours.
Lieferform/ Form of Delivery	Gewünschtes Kabel mit Mantelabschlüssen versehen, auf Spule gewickelt und in Plastikfolie (PE) eingeschweisst./ Required cable fitted with termination sheaths, coiled on drum, and packed and sealed in PE foil.
Hinweis/ Remark	Auf Kundenwunsch werden auch andere Leiterwerkstoffe geliefert. Die Bilder (Fig. 1/Fig. 2) sind Beispiele für ausgeführte Spulenformen, Magnetfluss-Sonden verschiedener Art und Grenzfrequenzen (z.B. Mirnov-Sonde) werden nach Spezifikation gemäß Kundenwunsch hergestellt./ Other conductor materials supplied on request. Samples of coil shapes already manufacured (Figs. 1 and 2). Custom-built magnetic flux probes of various shapes and limiting frequencies (e.g. Mirnov probe).

Entschlüsselung/Decoding

JK2L-E	Zweiadrige Signalleitung/Two-core signal line
JK2L-T	Zweiadrige Thermoelementleitung/Two-core thermocouple line
SK1L-E	Einadrige Signalleitung/Single-core signal line
SK1L-EU	Einadrige Signalleitung mit unterbrochenem Abschirmungsmantel (Anzahl Unterbrechungen pro Meter gemäss Kundenwunsch)/ Single-core signal line with interrupted sheath (number of gaps per metre according to specification)
SK2L-E	Zweiadrige Signalleitung/Two-core signal line
SK2L-T	Zweiadrige Thermoelementleitung/Two-core thermocouple line
0.3/0.5	Drahtdurchmesser beider Leiter in Millimeter/ Wire diameter of the two conductors in mm.
(Cu/Cu)	Leiterwerkstoff E-Cu/Conductor material E-Cu.
(NiCr/Ni)	Leiterwerkstoff gemäss DIN 43710/Conductor material acc. to DIN 43710
(NiCr)	Leiterwerkstoff (ca. 90 %Ni, ca. 10 %Cr) conductor material (ca. 90 %Ni, ca. 10% Cr)
MF 1	Umhüllung, Leiterdraht einmal mit Micafolie (Glimmer) umsponnen/ Sheath, conductor singly braided with mica foil.
GS	Nicht imprägnierte Glasseide (R-Glas), farblos/ Non-proofed glass silk, colourless.
2E/3E	Umhüllung, Leiterdraht zweimal bzw. dreimal mit Glasseide umflochten/ Sheath, conductor doubly or triply braided with glass silk.
1P 2P	Umhüllung, Leiterdrähte paarweise einmal bzw. zweimal mit Glasseide umflochten/ Sheath, conductors singly or doubly braided in pairs.
D	Verdrillung beider Leiterdrähte/Both conductors twisted.
25PH/50PH	25 bzw. 50 Verdrillungen pro 1 Meter Kabel/ 25 or 50 twists per metre cable.
A	Abschirmungsmantel geflochten/Sheath braided.
0.2	Drahtdurchmesser des Abschirmungsmantels in Millimeter/ Wire dia in mm of sheath.
(Cu)	Werkstoff des Abschirmungsmantels, E-Kupfer/ Material of Sheath, E-copper.
(SS)	Werkstoff des Abschirmungsmantels, Rostfreier Stahl (W.Nr. 1.4301 oder 1.4435)/ Material of sheath, stainless steel (W.No. 1.4301 or 1.4435).
(B75)	Mantel-Bedeckungsgrad ca. 75%/Cover of sheath appr. 75%.

Bestellcode für Sondenkabel/Order code for probe cable

Typ JK2L-E 0.5 (Cu/Cu)-GS 2E-2P-D 50PH A 0.2 (Cu) B75
Typ JK2L-T 0.3 (NiCr/Ni)-GS 2E-2P-D 50PH A 0.2 (Cu) B75

Typ SK2L-E 0.5 (NiCr)-MF1 GS 3E-A 0.2 (SS) B75
Typ SK2L-E 0.5 (NiCr/NiCr)-MF1 GS 2E-1P-D 25PH A 0.2 (SS) B75
Typ SK2L-T 0.5 (NiCr/Ni)-MF1 GS 2E-1P-D 25PH A 0.2 (SS) B75

FIG. 36 GENERAL REMARKS AND ORDER CODE